

© 2016

CECILIA MARGARIDA MENDES MOTTA

ALL RIGHTS RESERVED

EFFECT OF SURFACE FUNCTIONAL GROUPS ON CHONDROCYTE
BEHAVIOR USING MOLECULAR GRADIENTS

A Thesis

Presented to

The Graduate Faculty of The University of Akron

In Partial Fulfillment

of the Requirements for the Degree

Master of Science

Cecilia Margarida Mendes Motta

May, 2016

EFFECT OF SURFACE FUNCTIONAL GROUPS ON CHONDROCYTE
BEHAVIOR USING MOLECULAR GRADIENTS

Cecilia Margarida Mendes Motta

Thesis

Approved

Accepted

Advisor
Dr. Matthew L. Becker

Dean of the College
Dr. Eric J. Amis

Faculty Reader
Dr. Abraham Joy

Dean of the Graduate School
Dr. Chand Midha

Department Chair
Dr. Coleen Pugh

Date

ABSTRACT

Osteoarthritis (OA) is the most common articular disease and the most prevalent condition resulting in disability among the United States adult population. According to the U.S. Department of Health and Human Services, from 2010-2012, 52.5 million (22.7%) of adults aged ≥ 18 years had self-reported doctor-diagnosed arthritis, and 22.7 million (9.8%) reported arthritis-attributable activity limitation, which indicates not only an ethical, but also economic importance of this disease. OA is characterized by progressive loss of articular cartilage and leads to chronic pain and functional restrictions in the affected joint. Although current treatments are successful in some aspects to provide short-term pain relief and recovered joint mobility, their long term benefits remain elusive and there is still no cure for the disease. The limited capacity for treatment is mainly due to the cartilage's inability to repair itself. Regenerative medicine using tissue-engineered cartilage has the potential to address this issue, but a remaining challenge is the development of a feasible large scale cell expansion process, since during the expansion in monolayer cultures, chondrocytes undergo the process of dedifferentiation. Several surface-engineering approaches with bioactive factors and surface chemistry have been previously studied to look at increasing the interfacial interaction between the materials and cells. This project aimed to study the effects of various concentrations of surface functional groups on chondrocyte behavior. The cell proliferation and phenotype maintenance within continuously variable one-dimensional concentration gradients were examined. This

method included fabrication of functionalized gradients by a vapor deposition technique that provided a fast, efficient, and reliable strategy by incorporating a series of concentrations in single substrates. Finally, human primary chondrocytes density and cellular survival were studied as response of amine and hydroxyl terminal groups` concentrations.

Keywords: Cartilage, tissue engineering, cell expansion, surface functionalization, gradient concentrations.

DEDICATION

This master's thesis is dedicated to my family, to my advisor, to all members of the Becker group, and to my friends, for giving me all kinds of support through my Master`s.

ACKNOWLEDGEMENTS

First of all, I would like to thank the Brazilian government for my scholarship. The Science Without Borders program gave me the opportunity to explore an world of possibilities that I had never imagined I would have the chance to experience. I really hope one day I will be able to pay this investment back and help to make our Brazil a “better country for everyone”.

I would like to express my appreciation to my advisor, Dr. Becker, who has given me warm encouragement and support since the beginning of my Master`s program. He has been an admirable example of researcher, professor and human, with a tremendous intelligence and energetic disposition. Thank you for giving me the opportunity to be a Becker!

I also would like to thank Dr. Joy, as committee member and reader of my thesis, who has friendly spent his time to evaluate my work.

I would like to thank all the Becker group! I could not have asked to be part of a better research group! Each of you have a tremendous potential and a curiosity for science that inspired me through the course of my research. Thank you for all the support, the help, the knowledge and the friendship. I will never forget, “Two percent of a lot is still a lot!”.

Thank you all the academy for sharing your knowledge. With no doubt, each professor of the Department of Polymer Science from the University of Akron is a reference in his

research field. It has been an honor to get my Master`s degree in such a renewed Department.

I also would like to thank all my friends! My friends from childhood for believing I am still a smart one. My “Sem Censura” friends for listening to all my complains and making me feel like I am part of a group and I will never be alone. My Brazilian friends from the CsF for being my second family here in the United States. All the second year friends, you were all really important and without your support in the best and worst moments, I could not pass thought all the challenges of my Master`s.

Last but not least, I would like to thank my family. Theus, Fil, dad and mom, you are the reason of this achievement. Thank you for being so close even being so far. Thank you for given me inspiration, support and comfort. Thank you for believing on me. I love you!

TABLE OF CONTENTS

	Page
LIST OF FIGURES	x
LIST OF SCHEMES.....	xiv
CHAPTER	
I INTRODUCTION	1
II BACKGROUND.....	4
2.1 Osteoarthritis.....	4
2.2 Tissue engineering approach.....	8
2.3 Surface functionalization	11
2.4 Functional concentration gradient substrates (FCGS)	13
2.5 Objectives, motivation, innovation and hypothesis.....	15
III EXPERIMENTAL.....	16
3.1 Functional concentration gradient substrates (FCGS) fabrication.....	16
3.1.1 Chlorine-terminated FCGS fabrication.....	16
3.1.2 Azide-terminated FCGS fabrication	18
3.1.3 Amine-terminated FCGS fabrication.....	19
3.1.4 Hydroxyl-terminated FCGS fabrication	20
3.2 Surface analysis	22
3.2.1 Contact angle measurement	22
3.2.2 X-ray Photoelectron Spectroscopy	22

3.3 <i>In vitro</i> study	23
3.3.1 Cell isolation	23
3.3.2 Histological staining and immunohistochemistry.....	25
3.3.3 Proliferation assay.....	25
3.3.4 Phenotype maintenance assay	26
3.4 Statistical analysis	26
IV RESULTS AND DISCUSSION.....	27
4.1 Surface analysis	27
4.1.1 Contact angle	27
4.1.2 X-ray Photoelectron Spectroscopy	30
4.2 <i>In vitro</i> study	38
4.2.1 Proliferation assay.....	38
4.2.2 Phenotype maintenance assay	47
V CONCLUSIONS.....	56
VI SUMMARY.....	59
REFERENCES	60

LIST OF FIGURES

Figure	Page
<p>2.1: Human knee articular cartilage, Safranin O/fast green staining. (a) Normal cartilage: (1) Smooth surface; (2) cells in the tangential zone are small and flat; (4) The complete cartilage matrix stains with safranin O; (5) the tidemark is intact. (b) Mild OA: (1) Surface irregularities; (3) the staining with safranin O is reduced. (c) Severe OA: (1) Deep clefts in the surface; (2) cells have disappeared from the tangential zone; (3) cloning; (5) reduced to no staining of the matrix with safranin O. Reprinted from Lorenz <i>et al.</i>³ with permission from Elsevier. Copyright (2006).</p>	7
<p>2.2: Schematic representation of articular cartilage tissue engineering. In the process of tissue engineering, a few cells are isolated from a donor and expanded <i>in vitro</i> to achieve a population large enough to fill the defect. Then, they are seeded onto an appropriate three dimensional (3D) scaffold and implanted in the injured tissue to restore or replace the functions and properties. This figure was reprinted from Al-Rubeai <i>et al.</i> with permission from the American Institute of Chemical Engineers (AIChE). Copyright (2005).</p>	10
<p>4.1: (a) Scheme of contact angle points distribution across the substrates. The data was collected from five equidistant points on the surface at 5 mm intervals. (b) Gradient concentration profiles for chlorine (Cl), azide (N₃), amine (NH₂) and hydroxyl (OH) FCGS, and for chlorine uniform SAM and clean glass slide, measured by water contact angle. Static contact angle changed gradually across the surface of the FCGS as reflect of the increasing of the organosilane concentration. Changes in contact angle between terminal group substrates indicated that reactions were successfully completed. Deionized water static contact angle (mean ± S.E., n = 3).</p>	29
<p>4.2: Survey spectra (0-700 eV) from XPS for the chlorine surface concentration gradient. The peak at 201 eV, assigned as Cl_{2p}, verified that the chlorine was successfully tethered onto the silica wafer surface.</p>	31
<p>4.3: Survey spectra (0-700 eV) from XPS for the amine surface concentration gradient. The peak at 201 eV, assigned as Cl_{2p}, disappears, which indicates that the chlorine was quantitatively converted to amine functionality.</p>	32
<p>4.4: Survey spectra (0-700 eV) from XPS for the hydroxyl surface concentration gradient. The peak at 201 eV, assigned as Cl_{2p}, disappears, and a new peak evolves at 400 eV,</p>	

assigned as N_{1s}. It could be inferred that the chlorine functionalized surface was quantitatively converted to a hydroxyl functionalized surface.33

4.5: Peak fitting of XPS C_{1s} high resolution spectra for each gradient position on chlorine FCGS. The peak area increased along the substrate position, which implied that the concentration increased along the gradient. Decomposition was based on Gauss-Lorentz function.37

4.6: Surface concentration and surface coverage fraction as a function of position along the chlorine-terminated gradient surface, determined by XPS (n = 3).37

4.7: (a) Chondrocyte proliferation response as a function of hydroxyl concentration on hydroxyl FCGS. Cell number was collected at each sample position after days 1, 3 and 7 of culture. Values are represented as means ± standard error (S.E.), with P < 0.05 and n = 3. (b) Statistical analysis for cell proliferation on hydroxyl gradients data. Grey shaded boxes indicate significant differences for cell number from different positions in a same time point, or different time points in a same position (ANOVA with Tukey's, P < 0.05).41

4.8: (a) Human primary chondrocyte proliferation response in hydroxyl SAM substrate, with uniform concentration of 240 pmol/cm². Cell number was collected at each sample position after days 1, 3 and 7 of culture. Values are represented as means ± S.E., with P < 0.05 and n = 3. (b) Statistical analysis for cell proliferation on hydroxyl uniform SAM data. Grey shaded boxes indicate significant differences for cell number from different positions in a same time point, or different time points in a same position (ANOVA with Tukey's, P < 0.05).42

4.9: Immunofluorescent staining of actin (red), C5-maleimide (green) and nuclei (blue) for human primary chondrocyte culture on hydroxyl functionalized gradient surface after days 1, 3 and 7 of culture. Images were taken every 5 mm down length of the gradient. Scale bar = 20 μm.43

4.10: (a) Human primary chondrocyte proliferation response as a function of amine concentration on functionalized amine FCGS. Cell number was collected at each sample position after days 1, 3 and 7 of culture. Values are represented as means ± S.E., with P < 0.05 and n = 3. (b) Statistical analysis for cell proliferation on amine gradients data. Grey shaded boxes indicate significant differences for cell number from different positions in a same time point, or different time points in a same position (ANOVA with Tukey's, P < 0.05).44

4.11 (a) Human primary chondrocyte proliferation response in amine SAM substrate, with uniform concentration of 240 pmol/cm². Cell number was collected at each sample position after days 1, 3 and 7 of culture. Values are represented as means ± S.E., with P < 0.05 and n = 3. (b) Statistical analysis for cell proliferation on amine gradients data. Grey shaded boxes indicate significant differences for cell number from

different positions in a same time point, or different time points in a same position (ANOVA with Tukey's, $P < 0.05$).	45
4.12: Immunofluorescent staining of actin (red), C5-maleimide (green) and nuclei (blue) for human primary chondrocyte culture on amine functionalized gradient surface after days 1, 3 and 7 of culture. Images were taken every 5 mm down length of the gradient. Scale bar = 20 μm .	46
4.13: (a) Chondrocyte survival of each gradient position based on phenotype maintenance using CD14/CD90 ratios for days 3, 7 and 14 of culture on hydroxyl FCGS. Values are represented as means \pm S.E., with $P < 0.05$ and $n = 3$. (b) Statistical analysis for cell phenotype maintenance on hydroxyl gradients data. Grey shaded boxes indicate significant differences for cell number from different positions in a same time point, or different time points in a same position (ANOVA with Tukey's, $P < 0.05$).	50
4.14: (a) Chondrocyte survival of each gradient position based on phenotype maintenance using CD14/CD90 ratios for days 3, 7 and 14 of culture on hydroxyl uniform SAM surface, with uniform concentration of 240 pmol/cm^2 . Values are represented as means \pm S.E., with $P < 0.05$ and $n = 3$. (b) Statistical analysis for cell phenotype maintenance on hydroxyl gradients data. Grey shaded boxes indicate significant differences for cell number from different positions in a same time point, or different time points in a same position (ANOVA with Tukey's, $P < 0.05$).	51
4.15: Immunofluorescent staining of CD14 (red), CD90 (green) and nuclei (blue) for human primary chondrocyte culture on hydroxyl functionalized gradient surface after days 3, 7 and 14 of culture. Images were taken every 5 mm down length of the gradient. Scale bar = 20 μm .	52
4.16: (a) Chondrocyte survival of each gradient position based on phenotype maintenance using CD14/CD90 ratios for days 3, 7 and 14 of culture on amine FCGS. Values are represented as means \pm S.E., with $P < 0.05$ and $n = 3$. (b) Statistical analysis for cell phenotype maintenance on amine gradient data. Grey shaded boxes indicate significant differences for cell number from different positions in a same time point, or different time points in a same position (ANOVA with Tukey's, $P < 0.05$).	53
4.17: (a) Chondrocyte survival of each gradient position based on phenotype maintenance using CD14/CD90 ratios for days 3, 7 and 14 of culture on amine SAM surface, with uniform concentration of 240 pmol/cm^2 . Values are represented as means \pm S.E., with $P < 0.05$ and $n = 3$. (b) Statistical analysis for cell phenotype maintenance on amine uniform SAM data. Grey shaded boxes indicate significant differences for cell number from different positions in a same time point, or different time points in a same position (ANOVA with Tukey's, $P < 0.05$).	54
4.18: Immunofluorescent staining of CD14 (red), CD90 (green) and nuclei (blue) for human primary chondrocyte culture on amine functionalized gradient surface after	

days 3, 7 and 14 of culture. Images were taken every 5 mm down length of the gradient. Scale bar = 20 μm55

LIST OF SCHEMES

Scheme	Page
3.1: Reaction scheme of chlorine-terminated gradient fabrication. 4-chlorobutyldimethylchlorosilane was deposited on glass surface using a “vacuum away” confined channel vapor deposition method.....	17
3.2: Reaction scheme of azide-terminated gradient fabrication. Chlorine end group was substituted to azide end group in a S _N 2 reaction.	18
3.3: Reaction scheme of amine functionalized surface. The azide end group was reduced to amine end group via phosphinimine hydrolysis, using triphenylphosphine as the reduction agent.	19
3.4: Reaction scheme of hydroxyl functionalized surface. (a) The azide end group was converted to hydroxyl end group via an alkyne-azide cycloaddition reaction. Copper (II) sulfate was reduced by sodium ascorbate to produce the catalyst copper (I). (b) Proposed mechanism for the alkyne-azide cycloaddition reaction, from Himo <i>et al.</i> (2005).	21

CHAPTER I

INTRODUCTION

Osteoarthritis (OA) is the most common degenerative disease of the joints. It is a chronic condition that nowadays affects one in five adults in United States, and by 2030 it is estimated that 67 million Americans aged 18 years or older will present some kind of arthritis.¹ OA can affect any joint of the body and happens when the protective cartilage that covers the end of the bones wears down, causing pain, swelling, discomfort, and difficulty of movement. In the worst case, bones can break down, developing an inflammatory process followed by more pain and disability.² Although this becomes more common with age, it results from a combination of risk factors, including obesity, overuse of joints through sports or other common daily activity, previous trauma and genetic disposition.³ OA symptoms often hinder work and social life, with high economical costs, and it can affect the patient`s overall health, since the pain leads to reduced mobility and weight gain, development of diabetes, heart disease, and increased risk of falls and fractures.⁴ Due to inability of cartilage to repair itself, treating these patients is a challenge. While there is still no cure for this disease, current treatments are available to manage the symptoms, such as analgesics, nonsteroidal and corticosteroids anti-inflammatory drugs, injections of hyaluronic acid (a natural joint lubricant fluid and shock absorbent), and surgery.⁵

In the case of knee joints, for example, it has been estimated that 12% of Americans aged 25 years or older have clinical signs and symptoms of OA.⁶ It starts as a lack or loss of the articular cartilage at the end of the femur and tibia, and progresses into involvement with surrounding tissues and synovial fluid. In more severe cases, surgical treatments may be the only solution. Less invasive procedures include chondroplasty, microfractures of the underlying bone, osteochondral autograft transplant, amongst others. These methods usually provide only temporary relief for the pain.⁷ The most commonly performed procedure in advanced OA is the partial or total replacement of the weight-bearing surfaces of the joint by prosthesis of polymeric and metallic parts. Although this technique has evolved and improves pain relief for many patients, it does not resolve the prior functional limitations, and it can bring significant complications for being a highly invasive procedure. As an example, the currently used materials have a tendency to fail after long term usage if vital requirements are not met, such as modulus close to the bone, and high wear and corrosion resistance.⁸

To overcome these complications, nonsurgical and less invasive alternatives are appealing, especially the injection of isolated mesenchymal stem cells and bone marrow concentrates.⁶ The matrix-induced autologous chondrocytes implantation has demonstrated encouraging clinical outcomes, with evidence of tissue regeneration. Carticel®, for example, is a FDA approved treatment that uses the patient's own cells to repair knee cartilage injuries, forming a new hyaline-like cartilage, with properties similar to normal cartilage.⁹ However, these treatments are not promising for patients with moderate to severe OA, and clinical outcomes have observed the incidence of graft hypertrophy (a protuberance of tissue that grows above the adjacent native cartilage) and

bone marrow edema in many patients in postoperative phase, which unfortunately would require revision surgeries.⁷

Overall, several therapies for osteoarthritis manage this chronic disease, but the need of development for an effective and safe treatment encourages the medical society to promote additional studies. Regenerative medicine using matrix-induced autologous chondrocyte implantation and/or tissue-engineered cartilage have the potential to resolve this issue by developing a cell-based biomaterial set up to restore or replace the damaged joint.¹⁰

This project is focused on the cell expansion step for cartilage tissue engineering. We aimed to study the effect of various concentrations of hydroxyl and amine surface functional groups on chondrocyte behavior. The approach included fabrication of one dimensional functional concentration gradient substrate (FCGS) by a vapor deposition method¹¹ and study of human primary chondrocyte proliferation and phenotype maintenance potential within functional groups of varying surface concentrations.

In Chapter II of this thesis, the unmet medical need for effective solutions to repair osteoarthritis and the current treatments are briefly introduced, as well as the objective and hypothesis of this project.

In Chapter III, the methodology for the synthesis and characterization of the FCGS substrates are described, along with the procedure for cell culture and immunofluorescence studies in order to verify chondrocyte proliferation and phenotype.

In Chapter IV, the results of this study are presented and discussed.

Chapter V summarizes the conclusions.

Chapter VI summarizes this work.

CHAPTER II

BACKGROUND

2.1 Osteoarthritis

Osteoarthritis (OA) is the most common articular cartilage disease and the most prevalent condition leading to disability among the adult population in the United States of America.¹²⁻¹⁴ Data from 2010-2012, compiled by the U.S. Department of Health and Human Service, indicates that 52.5 million (22.7%) adults aged ≥ 18 years had self-reported doctor-diagnosed arthritis, and 22.7 million (9.8%) reported arthritis-attributable activity limitation.^{1, 14} The economic costs of OA are high, including the procedure costs and treatment, adaption for a new life style and loss of work productivity. Symptomatic knee osteoarthritis, for example, leads to \$27 billion in medical-care costs annually in the USA, which indicates not only an ethical, but also economic importance of this disease.¹⁵⁻¹⁶

OA is characterized by the progressive loss of articular cartilage and leads to chronic pain and functional restrictions in the affected joint.¹⁷ Different factors can be involved in the development of the disease, specially ageing, traumatic events, genetic disposition and obesity.¹⁷ Unfortunately, articular cartilage has an avascular and aneural nature, which results in poor healing and a limited capacity for self-repair.³ Only small defects with minimal loss of extracellular matrix can be regenerated. Further, osteoarthritis changes are usually diagnosed in the advanced stage, when the disease has progressed and a

pronounced alteration of the joint causes pain, and the changes can be detected radiographically. At this point, treatment becomes particularly difficult.^{3, 18}

Articular cartilage is a complex connective tissue that covers the surface of bones in synovial joints and promotes load-bearing resistance and enables low-friction articulation. Its viscoelastic and compressive properties are provided by the extracellular matrix (ECM), composed mainly of water, collagen type II and the large proteoglycan aggrecan.¹⁹ Due to the lack of blood vessels and nerves, nutrients and cellular repair components must rely on diffusion from the synovial fluid. As a result, features and degeneration of the tissue leads to an imbalance between anabolic and catabolic products, and enhances still more the degradation process.^{10, 20}

The mechanism and physiological process of articular cartilage degradation is not fully understood, but it is assumed that at the initial stage, the matrix-network changes at the molecular level. The water content increases and an overexpression of matrix-degrading enzymes causes the matrix to lose collagen type II and proteoglycan, leading to reduced stiffness of the cartilage.²¹ The chondrocytes respond by enhancing proliferation and metabolic activity. In the last stage, the cells are not able to keep the high repair activity. Due to the loss of cartilage tissue, the subchondral bone reacts with fibrillation and formation of cysts, or osteophytes, of which the significance is still not known, but distinguishes OA from other arthritis.²² It is also established that the degeneration process is spatially diverse in the different cartilage zones, with chondrocyte cells expressing different activity levels.³

The progress of OA can be tracked by morphological changes in the tissue. Healthy hyaline cartilage has a smooth surface and is usually white, elastic and firm. It has four

layers. The superficial layer has flat cells arranged parallel to the joint. The intermediate layer has round cells that form columns perpendicular to the surface, embedded in ECM, which stains with safranin O, a common marker for cartilage proteoglycan. The radial zone is a border between non-calcified and calcified cartilage, and the last zone, which is a tidemark before the subchondral bone, comprehends calcified cartilage. With the advance of OA, the cartilage shows discoloration and becomes dull and irregular. The surface is rough and sometimes new blood vessels can be found. It loses thickness, and in progressive stages full-thickness areas can be observed, exposing the subchondral bone. The tissue becomes disordered, cells become fibroblast-like and the ECM loses proteoglycan, no more standing for safranin O (Figure 2.1).³

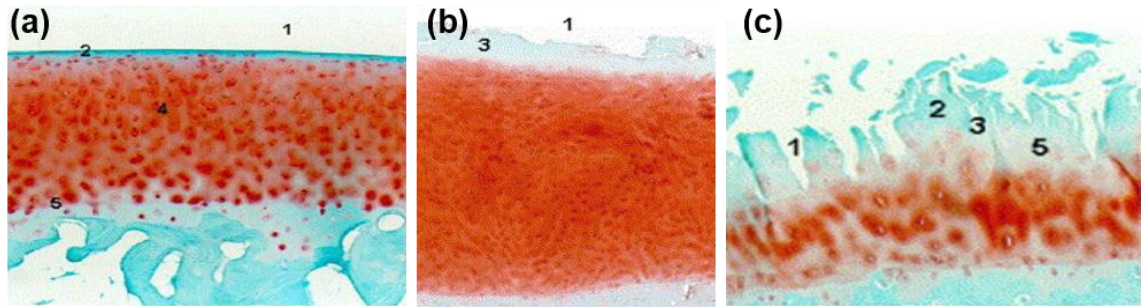


Figure 2.1: Human knee articular cartilage zones, Safranin O/fast green staining. (a) Normal cartilage: (1) Smooth surface; (2) cells in the tangential zone are small and flat; (4) The complete cartilage matrix stains with safranin O; (5) the tidemark is intact. (b) Mild OA: (1) Surface irregularities; (3) the staining with safranin O is reduced. (c) Severe OA: (1) Deep clefts in the surface; (2) cells have disappeared from the tangential zone; (3) cloning; (5) reduced to no staining of the matrix with safranin O. Reprinted from Lorenz *et al.*³ with permission from Elsevier. Copyright (2006).

The limited ability for articular cartilage to repair itself makes it necessary the intervention of surgical treatments.²³ Current clinical treatments include debridement of loose chondral flaps; mosaicplasty and transplants to fill the defect with healthy cartilage pieces; microfracture or stimulation of the intrinsic subchondral bone, and autologous chondrocyte implantation.¹⁰ Although these techniques are successful in some aspects to provide short-term pain relief and recovered joint mobility, each of them has limitations and their long term benefits remain elusive.^{7, 24-27} Marrow stimulation, for example, results in fibrocartilage, and autografts suffer from lack of integration. Therefore, the resulting repaired tissue does not exhibit the same biomechanical properties as the native articular cartilage and eventually breaks down, requiring additional treatments and, in the worse scenario, a total joint arthroplasty is the remaining solution.²⁴ The lack of a well-established clinical solution to this problem has given attention to the development of new approaches involving bioengineered constructs to mimic the complex native articular cartilage composition and architecture, providing adequate cellular environment to favor the tissue long-term regeneration.²⁸

2.2 Tissue engineering approach

An alternative approach for the repair of damaged articular cartilage comes from the tissue engineering therapy, that focus on developing a biological substitute to restore or replace the structure and function properties of the damaged tissue. The avascular nature of cartilage, with only one cell type, gives the impression to be an easy construct, but it is still allusive the development of a clinically relevant and functionally engineered cartilage tissue for load bearing applications.^{10, 29}

In the process of articular cartilage tissue engineering, the first phase is the isolation of a few cells to be expanded *in vitro* (Figure 2.2). These cells can be taken from a donor (allogeneic), or in the best case from the own patient (autologous), and they can be mature cells (chondrocytes), or immature cells (mesenchymal stem cells). The expanded cells are seeded onto an appropriate three dimensional scaffolds and implanted in the injured tissue.²⁹ Although this technology has been widely evolved since the first approach, from Vacanti *et al.* (1991), it still faces many challenges related to the choice of the best cell source, the *in vitro* culture environment conditions, biomaterial design, and remain difficult to incorporate neo-cartilage with adjacent healthy tissue. In addition, one of the main problems is the development of a feasible large scale cell expansion process. Adult chondrocytes have a limited ability to maintain their phenotype expression and dedifferentiate after extensive expansions *in vitro*. Therefore, it is fundamentally important to optimize the cell culture conditions.³⁰

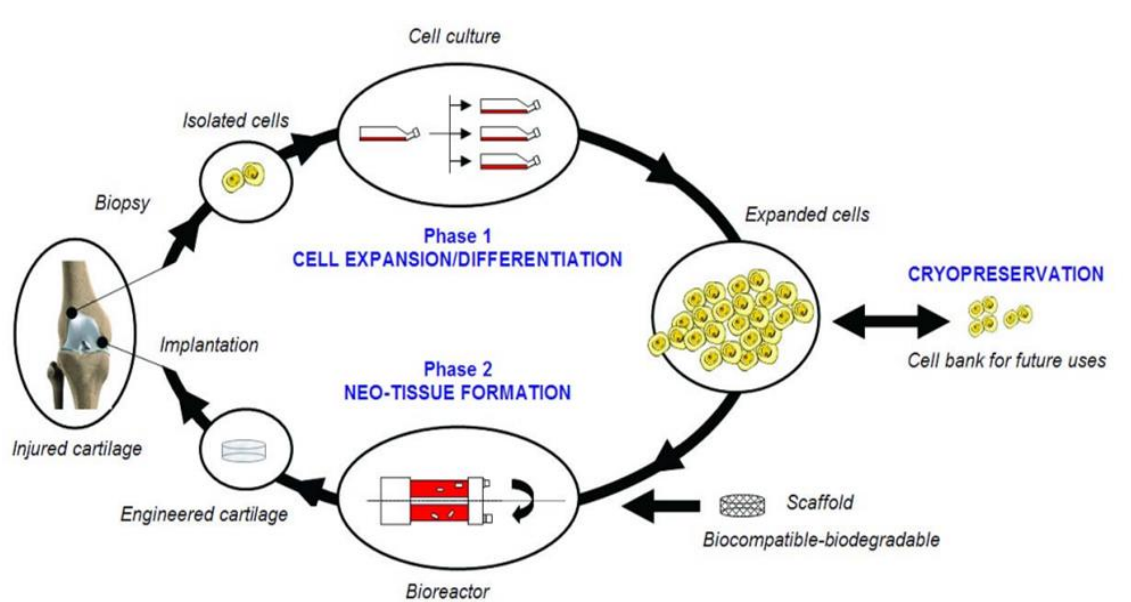


Figure 2.2: Schematic representation of articular cartilage tissue engineering. In the process of tissue engineering, a few cells are isolated from a donor and expanded *in vitro* to achieve a population large enough to fill the defect. Then, they are seeded onto an appropriate three dimensional (3D) scaffold and implanted in the injured tissue to restore or replace the functions and properties. This figure was reprinted from Al-Rubeai *et al.* with permission from the American Institute of Chemical Engineers (AIChE). Copyright (2005).

During the expansion in monolayer cultures, chondrocytes isolated from their tissue-specific extra-cellular matrix undergo the process of dedifferentiation. After the suspension in medium, cells adhere at the bottom of the culture flask, in a monolayer, and after a few days they start to change their appearance to a fibroblast-like morphology.³¹ It is believed that this process is mediated by the formation of actin stress fibers induced when cells spread to adhere onto the substrate.³⁰ Chondrocytes also switch the synthesis of cartilage matrix components. Articular chondrocytes in their natural environment produce a matrix that confers tensile strength and flexibility to the tissue, whereas growth plate chondrocytes (or hypertrophic chondrocytes) produce a matrix capable of undergoing mineralization. Therefore, cultured chondrocytes start to produce collagens types I and III instead of collagen type II, and low molecular weight proteoglycans (versican) instead of large aggregations of proteoglycans.³² In addition, chondrocytes derived from articular cartilage biopsies have a limited proliferative potential, and usually the conditions that favor the cell number increase are not those that favor phenotype maintenance.³³

Facing this important limitation on the expansion potential of adult chondrocytes for tissue engineering applications, efforts are needed aiming to optimize *in vitro* monolayer cell culture methods for neo-cartilage fabrication.

2.3 Surface functionalization

Properties of biomaterial substrates, such as surface energy, roughness and chemistry have been linked to cell behaviors such as adhesion, morphology and proliferation for different cell lines.³⁴ Several studies have suggested that alterations in one or more of these parameters can affect, for example, the biological stimuli for phenotype-specific gene

expression and functional differentiation of different mesenchymal stem cells (MSC) lineages.³⁵⁻³⁶ In most of the cases, the stimuli relies on biological intervention, such as growth factors and cytokines, but Curran *et al.* (2006) proposed that the stimuli could be also driven from specific substrate surface modifications. By that time, self-assembled monolayers (SAMs) have already been used to study the effects of different surface chemistries on cell behavior, since with SAMs it was possible to create well-defined, replicable and well-characterized surfaces with a range of chemical functionalities.^{35, 37-39} By chemically modifying surfaces of glass-slides, different functionalities to the substrate are promoted, such as methyl (-CH₃), hydroxyl (-OH), and amine (-NH₂), all of them naturally found in biological systems. This technique for surface modification could ensure that the surface chemistry was the only variable within the substrates.³⁷ Their results demonstrated that surface chemistry has influence on cell behavior, as they presented diverse cell viabilities for different functional groups on the same substrate.

Another powerful *in vitro* system that has been explored and allowed significant control over surface chemical properties is SAMs of ω -functionalized alkanethiols on gold. J. E. Phillips *et al.* (2010) have analyzed the influence of four different biomaterial surface chemistries on human MSC differentiation along osteogenic, adipogenic and chondrogenic lineages, examining several phenotypic features, such as adhesion, morphology and long-term growth. During the hMSC differentiation into chondrocytes, different functionalized surfaces have shown to be more favorable for cartilage-specific phenotype induction. For example, type II collagen was upregulated on amine and methyl surfaces, compared to hydroxyl SAMs, while the opposite effect was observed for aggrecan, which was upregulated on hydroxyl compared to amine and methyl SAMs.³⁵ The variation on

chondrogenic gene expression of cartilage ECM components (collagen and aggrecan) in different surface functionalities, confirmed the importance of surface chemistry investigation for cell culture.

2.4 Functional concentration gradient substrates (FCGS)

As introduced before, surface chemistry has an important role in biological processes, including adhesion, protein adsorption, and cell attachment, growth and proliferation. FCGS have a high potential when studying surface chemistry because they enable the extrapolation of a continuous range of concentrations in one single substrate, allowing a rapid, efficient and precise platform for quantitative analysis of the phenomena to be studied.⁴⁰⁻⁴¹ Moreover, cell behavior on different surface chemistries has been extensively studied on discrete samples, but FCGS allows study of the cell response to a wide range of concentrations on single-substrates and this approach gives opportunities to observe transition regions or other phenomena that would be undetected in a discrete format.⁴¹

Different methods to generate SAM FCGS have been widely explored, such as microcontact and electric potential stamping, free diffusion, ultra-violet (UV)-induced oxidation, plasma and corona discharge, but preferential method is chosen according to the desired control of the slope and functional properties, batch to batch reproducibility, and the versatility of the chemical groups on the surface. Liquid and vapor deposition involve quite simple devices and are appropriate when a gradual change in the functionality present is desired, but as liquid diffusion requires compatibility between the substrate and the solvent, many times the vapor deposition becomes more versatile.¹¹

The most common chemistries employed for generating surface FCGS involve the attachment of organosilanes to silica or thiols to gold substrates. For the production of one single-component gradient, for example a hydrophobic component deposition on a hydrophilic substrate, the vapor deposition method can be used to control the motion of dilute solution liquid drops on surfaces, manipulating the grafting density and producing gradients on a micrometer length scale.⁴⁰ Ma *et al.* adapted a simple “vacuum away” confined channel vapor deposition method that allows the generation of linear gradient chemical concentrations profiles on silicon and glass substrates. They reported the versatility of the method for a range of functionalities, with good control over the concentrations profiles. Thereby, it has god potential to study the concentration-dependent effects of different functional species on cell behavior, aiming to enhance cell expansion for biomedical engineering applications.¹¹

In this method, silicon and glass slide substrates are pretreated with ultraviolet light generated ozone to clean the surface from organic contaminants. A Teflon® support, with place for chlorosilane reservoir and the glass substrate, is inserted into a rectangular glass tubing, which is placed in a sealed metal chamber. Dynamic vacuum is applied from the side nearest the reservoir and, after the reaction, methanol is injected through the opposite side to quench the diffusion process.

The expected profile of the FCGS in this system can be described according to Fick’s diffusion laws:

$$J = -D \frac{\partial c(x,t)}{\partial x} \quad (1)$$

$$\frac{\partial c(x,t)}{\partial t} = -D \frac{\partial^2 c(x,t)}{\partial x^2} \quad (2)$$

It is considered that for this boundary case, at position $x=0$ the concentration is constant, $\partial c(0)/\partial t=0$, and at position $x=\pm\infty$ the concentration is almost zero, $c(\pm\infty)=0$. Then, for relatively short distances, $x\ll 2(Dt)^{1/2}$, and the solution for equation 2 can be simplified as

$$c(x,t)=c(0)[1-x/(Dt\pi)^{1/2}] \quad (3)$$

Where concentration has almost a linear relationship with distance.¹¹

2.5 Objectives, motivation, innovation and hypothesis.

This thesis summarizes our effort to optimize chondrocyte cell expansion for cartilage tissue engineering. Although functionalized surfaces have been previously explored to study cell behavior, chemical concentrations have not been widely studied. In our approach, hydroxyl and amine gradient concentration substrates were probed to investigate chondrocyte proliferation and phenotype maintenance behavior in monolayer culture.

CHAPTER III

EXPERIMENTAL

3.1 Functional concentration gradient substrates (FCGS) fabrication

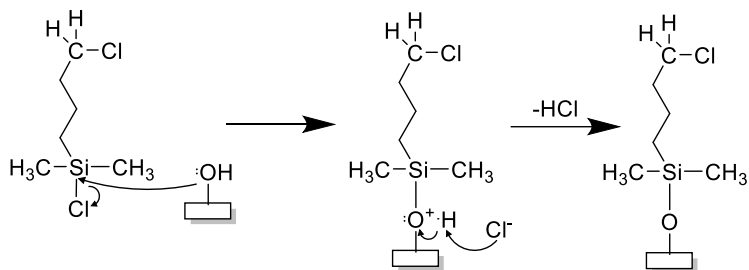
For creation of FCGS, a “vacuum away” confined channel vapor deposition method was used to fabricate linear gradient chemical concentrations profile, followed by sequential “click reactions” carried out for generation of different functionalities.¹¹

3.1.1 Chlorine-terminated FCGS fabrication

Microscope glass coverslips (2.5 cm², Fisher Scientific) were used as substrates for gradient fabrication. After washing with methanol, toluene and methanol, and blown dry with nitrogen, substrates were pretreated with ultraviolet light generated ozone (UVO; Jelight Company Inc. Model No. 42A) for one hour to remove organic contaminants from the surface. A Teflon support, with a channel for a chlorosilane reservoir (1.5 x 2.5 x 1.1 cm) and the glass substrate (7.5 x 2.5 x 1.0 cm), was inserted into a rectangular glass tubing (30 x 2.5 x 1.3 cm), which was intern in a sealed metal chamber. Dynamic vacuum (4 mPa) was pulled from the side nearest the reservoir and away from the substrate and, after a defined reaction time, methanol was injected through the opposite side to quench the diffusion process.

A solution of 10% 4-chlorobutyldimethylchlorosilane (150 μ L, neat in the Teflon reservoir) was used as the chemical source for the fabrication of chlorine-terminated FCGS

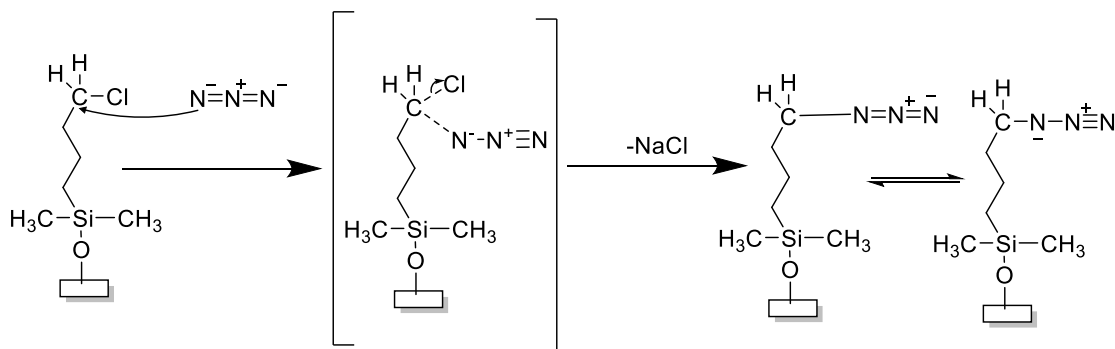
(Scheme 3.1). Vapor deposition was performed for 10 seconds, and substrates were washed successively with methanol, toluene, and methanol, and blown dry under nitrogen. Samples were stored in a vacuum desiccator at room temperature until used.



Scheme 3.1 Reaction scheme of chlorine-terminated gradient fabrication. 4-chlorobutyldimethylchlorosilane was deposited on glass surface using a “vacuum away” confined channel vapor deposition method.

3.1.2 Azide-terminated FCGS fabrication

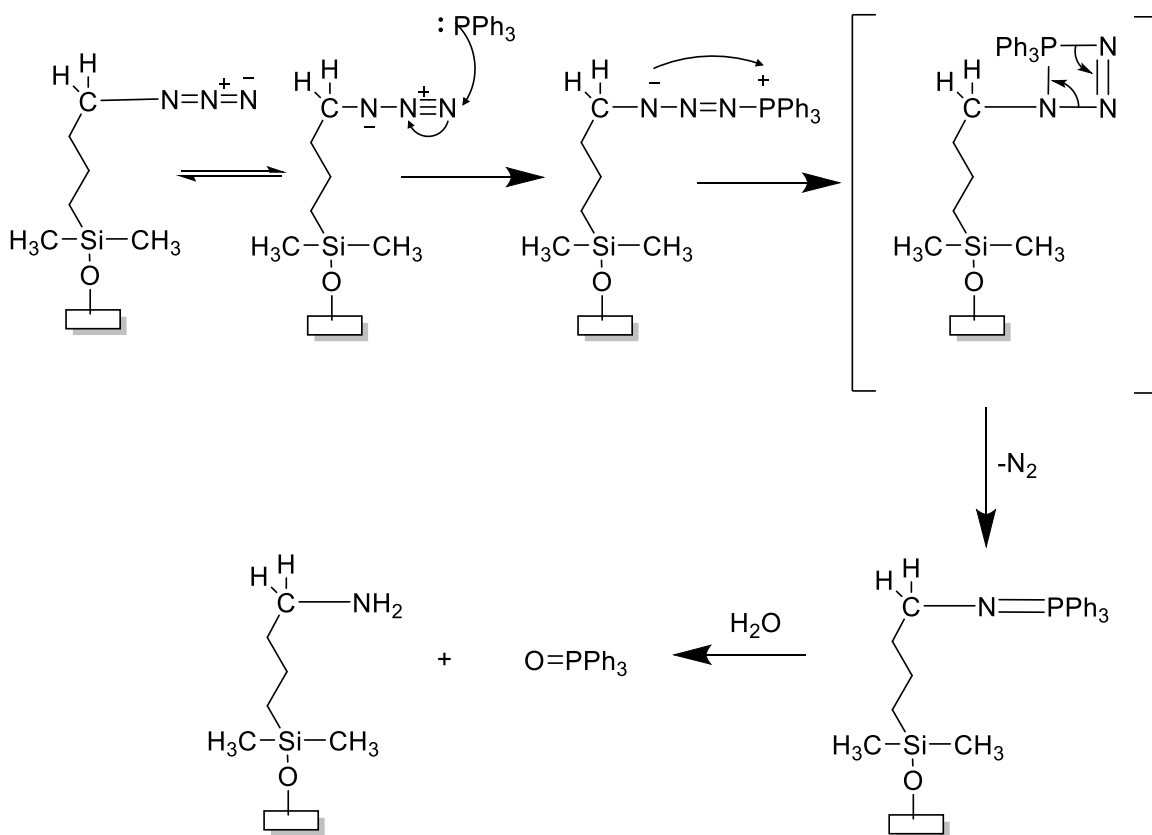
After the chlorine FCGS fabrication by vapor deposition, a S_N2 substitution of chlorine end group with azide end group was carried out (Scheme 3.2). The chlorine FCGS substrates were incubated in a solution of NaN_3 (0.2 g, 61 mM) in dimethylformamide (HPLC grade, 50 mL) solution with a small amount of 18-crown-6 as a phase transfer-catalyst, at 65 °C. After 48 hours, slides were removed, washed with methanol, toluene and methanol, and blown dry under nitrogen. Samples were stored in a vacuum desiccator at room temperature until used.⁴²



Scheme 3.2: Reaction scheme of azide-terminated gradient fabrication. Chlorine end group was substituted to azide end group in a S_N2 reaction.

3.1.3 Amine-terminated FCGS fabrication

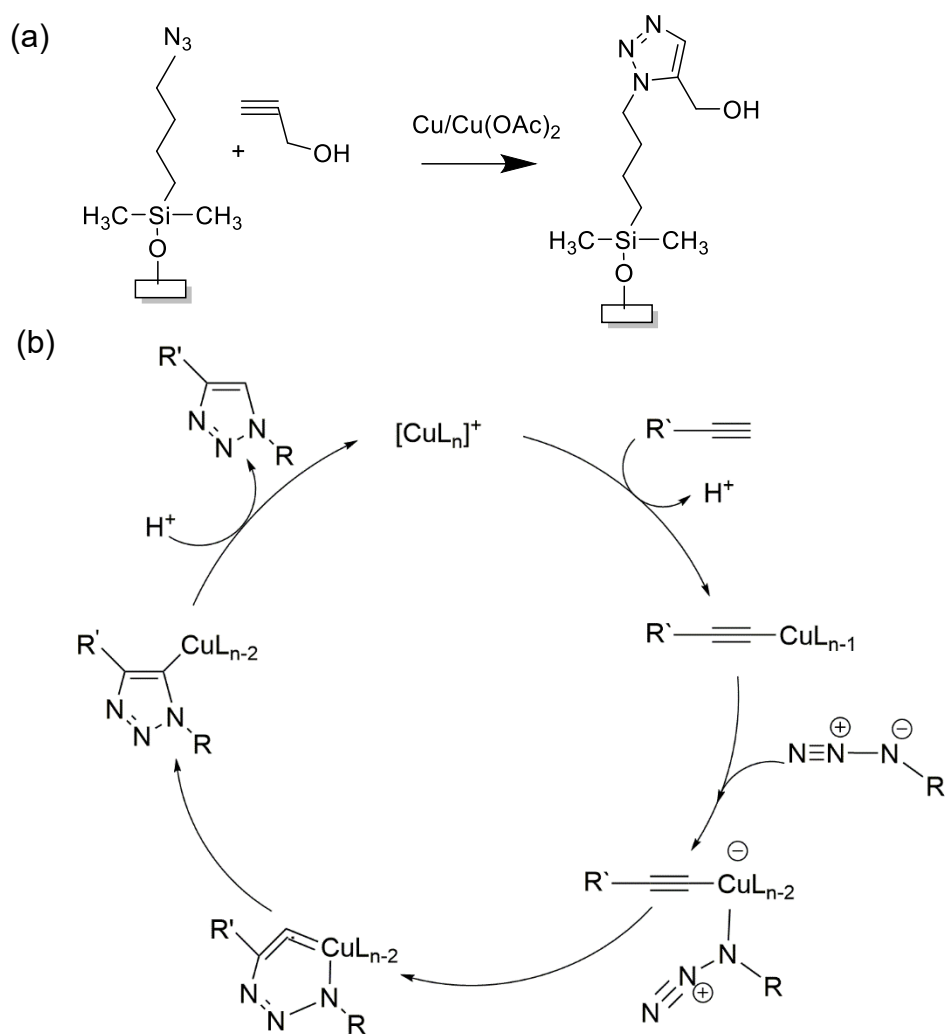
For the amine-terminated FCGS fabrication, azide-terminated FCGS was incubated in a solution of PPh_3 (0.78 g, 3 mM) in H_2O (54 μL , 3 mM) and THF (30 mL) at room temperature for 12 hours (Scheme 3.3). The substrates were then washed with methanol, toluene and methanol and blown dry under N_2 . Samples were stored in a vacuum desiccator at room temperature until used.



Scheme 3.3: Reaction scheme of amine functionalized surface. The azide end group was reduced to amine end group via phosphinimine hydrolysis, using triphenylphosphine as the reduction agent.

3.1.4 Hydroxyl-terminated FCGS fabrication

For the hydroxyl-terminated FCGS fabrication, a copper-catalyzed alkyne-azide cycloaddition was carried out (Scheme 3.4). Azide-terminated FCGS slides were immersed into 3-butyn-1-ol (60 μ L, 0.79 mM)/CuSO₄ (60 mg, 0.37 mM)/ Sodium ascorbate (120 mg, 0.60 mM)/ THF (15 mL)/ H₂O (15 mL), at room temperature for 48 hours. To remove the residual copper catalyst, the substrates were washed in EDTA (10 mmol/L, pH = 7) solution for 2 hours, then washed with methanol, toluene and methanol, and blown dry under N₂. Samples were stored in a vacuum desiccator at room temperature until used.



Scheme 3.4: Reaction scheme of hydroxyl functionalized surface. (a) The azide end group was converted to hydroxyl end group via an alkyne-azide cycloaddition reaction. Copper (II) sulfate was reduced by sodium ascorbate to produce the catalyst copper (I). (b) Proposed mechanism for the alkyne-azide cycloaddition reaction, from Himo *et al.* (2005).

43

3.2 Surface analysis

A well-defined surface characterization of FSGS has an important role for biological applications, in order to standardize and quantify the results. In this study, contact angle and X-ray Photoelectron Spectroscopy (XPS) were chosen to analyze surface energy and composition.

3.2.1 Contact angle measurement

Advancing contact angles were measured using an Advanced Goniometer (Rame-Hart Instrument Co., Model 500) at room temperature, using 2 μL ($18 \text{ M}\Omega \text{ cm}^{-1}$) ultrapure water as the probe fluid and analyzed by a drop shape analysis method (ImageJ, free download from <http://imagej.net/Downloads>). The data was collected from five equidistant points on the surface of the substrates at 5 mm intervals, and standard uncertainty was determined by standard error between measurements on three samples prepared under identical conditions.

3.2.2 X-ray Photoelectron Spectroscopy

The concentration profile and functionality of engineered substrates were determined by XPS measurements, performed on a PHI 5000 Versa Probe II Scanning XPS Microprobe spectrometer, using silicon wafers as substrates (Si[100], one side polished, Silicon Quest Int., cut to 25 x 25 mm). The X-ray source was monochromated Al K, scanning over a binding energy range of 0 to 700 eV with dwell time of 100 ms. The analyzer pass energy was 117.4 eV for the survey spectra and 20 eV for the high resolution C_{1s} scan. Each spectra was collected over a 300 x 700 μm area of the samples. Peak area was

analyzed and atomistic concentrations were calculated with Multipak software using Gauss-Lorentz function and assuming a linear background.

3.3 *In vitro* study

The well-defined FCGS samples were used to examine the effect of amine and hydroxyl concentration on cellular proliferation and phenotype maintenance from primary human chondrocytes isolated from OA cartilage.

3.3.1 Cell isolation

Institutional Review Board (IRB) approval was obtained at each of the institutions involved for the use of human tissue. For the amine functional group study, chondrocyte cells were isolated from the tibial plateaus and femoral condyles of a single patient undergoing total knee arthroplasty for osteoarthritis, and for the hydroxyl functionalized group study, chondrocytes were isolated from the femoral head of a single patient undergoing hip arthroplasty for degenerative arthritis. Both patients were male and in their 50`s years of age.

Under a laminar flow hood, joints were placed in a disposable dish containing phosphate buffered saline (PBS; Invitrogen, Grand Island, NY) solution supplement with 0.2 mg/mL primosin. When necessary, mesenchymal repair tissue was removed with scissors and scalpels to clear the cartilaginous layer completely. Full-thickness strips of cartilage were obtained by cutting across the layers, excluding the subchondral bone. The strips of cartilage were placed into a dish containing 4 mg mL⁻¹ collagenase type II (230 u/mg; Worthington Biochemical Corporation; Lakewood, NJ) in Hank`s buffered salt

solution Reduced Serum Eagle's Minimum Essential Media (Opti-MEM® I Reduced Serum Media (1x), Gibco; Invitrogen, Grand Island, NY), and diced into about 1-3 mm³ pieces, using scalpels. The pieces of cartilage were transferred to a 50 mL Erlenmeyer, and placed on a stir plate in a humidified 5% CO₂-balanced air atmosphere at 37 °C for 4 hours, stirring at low speed. The solution was then transferred to a 50 mL polypropylene tube (without chunks) and, again, centrifuged for 3 minutes at 3000 rpm. The supernatant was discarded. The pellet was resuspended in PBS to wash cells from collagenase and, again, centrifuged for 3 minutes at 3000 rpm. This process was repeated once. Cells were resuspended in a complete chondrocyte medium (Opti-MEM supplemented with 0.1 mg/mL primosin and 0.05 mg/mL ascorbate) and the suspension was passed through a 22 mm diameter ~80 µm stainless steel syringe filter to remove cellular debris. Cells were placed in a Corning® 75 cm² rectangular canted neck cell culture flask (Corning, NY), and precultured in a humidified 5% CO₂-balanced air atmosphere at 37°C for 24 hours. After the preculture phase, supernatant was aspirated and cells were treated with 5 mL 0.05% trypsin, for 9 minutes, gently shaking to release cells. The solution was transferred to a 15 mL polypropylene tube, centrifuged for 3 minutes at 3000 rpm, aspirated and washed with PBS. Cells were resuspend in 5 mL of complete chondrocyte medium. Trypan Blue was used to count viable cells in a hemocytometer, and cells were seeded at the engineered FGC substrates, previously sterilized with ethylene oxide, in a density of 3000 cells/cm² in 6-well plates, and incubated in a humidified 5% CO₂-balanced air atmosphere at 37 °C for 24 hours according to the period of interest for each assay, with medium changed every day. ^{33, 44}

3.3.2 Histological staining and immunohistochemistry

After each incubation period, the supernatant was aspirated and samples were fixed with 3.7% warm formaldehyde (Acros Organics; Hampton, NH) solution for 9 minutes, at 37 °C. The solution was aspirated and a new solution with 0.5% TritonX-100 (Acros Organics) in CS buffer (0.1 M PIPES, 1 mM EGTA, and 4% (w/v) 8000 MW polyethylene glycol, pH=6.9) was used to permeabilize cells, incubating one more time at 37 °C for 9 minutes. Samples were rinsed 3 times with CS buffer solution at room temperature, for 5 minutes each wash, followed by a soak in 0.05% fresh sodium borohydride (Acros Organics) in PBS, used to quench activity and remove excess formaldehyde, and incubated at room temperature for 10 minutes. Samples were washed 3 times with PBS and treated for histological staining and immunohistochemistry.⁴²

3.3.3 Proliferation assay

Samples were observed after 24 hours, 3 days and 7 days incubation periods, for actin, C5-Maleimide and nuclei organization. Samples were blocked from non-specific binding with 5% donkey serum (Invitrogen) in PBS, incubated at 37 °C for 20 minutes, and stained with rhodamine phalloidin (Invitrogen, 1:200 dilution) for one hour. After rinsing three times with PBS, samples were stained with Alexa Fluor 488 C5-maleimide (Invitrogen, 1:200 dilution) for one hour. DAPI (Sigma, 1:1000 dilution) was used to stain the cell nuclei, for 20 minutes, followed by three times wash in PBS. Samples were imaged on a IX81 microscope (Olympus).⁴²

3.3.4 Phenotype maintenance assay

For phenotype maintenance assay, samples were fixed as previously mentioned after 3 days, 7 days and 14 days. After 30 minutes incubation with 0.1% donkey serum and 0.01% sodium azide (Acros Organics) in PBS, samples were blocked with donkey serum 10% in PBS for 1 hour, at 37 °C. Samples were then incubated with CD 14 (SC9150; Santa Cruz Biothechnology, Santa Cruz, CA; 1:100 dilution) and CD 90 (SC6071, Santa Cruz; 1:100 dilution) primary antibodies overnight, and stained with appropriate Alexa Fluor secondary antibodies (anti-rabbit Alexa Fluor 546 and anti-goat Alexa Fluor 488; Invitrogen; 1:400 dilution) and DAPI (1:1000 dilution) for 1 hour, washed three times with PBS and viewed. CD14/CD90 ratio was obtained by dividing the fraction of cells expressing the surface marker CD14, by the fraction of cells expressing CD90, and it was used to quantify phenotype maintenance. Samples were imaged on a IX81 microscope (Olympus).⁴²

3.4 Statistical analysis

All experiments were conducted three times ($n = 3$), using 3 gradient substrates and 3 uniform SAM substrates. Samples were recorded at 4X montage for statistical analysis of each of the 5 concentration regimes along the gradient. CellSens (Olympus Corporation), was used to count cell number, and number of cells expressing CD14 and CD90. Randomly picked images ($n = 5$) were taken at 40X magnification at each concentration regime along the FCGS for qualitative analysis. All quantitative data is presented as the average \pm standard error and significance is performed as means of one-way analysis of variance (ANOVA), with P-value set as less than 0.05.⁴²

CHAPTER IV

RESULTS AND DISCUSSION

4.1 Surface analysis

The fidelity of our fabrication methods was assessed by characterization of the substrates by contact angle measurements and XPS.

4.1.1 Contact angle

In this current study, a “confined away” channel vapor deposition method was used to create linear gradient chemical concentration profiles of hydroxyl and amine functional groups on glass cover slide substrates. The chemical source (organosilane) and substrate were placed in a sealed chamber and a dynamic vacuum pulled from the opposite direction to create the diffusion concentration gradient. This method, previously adapted from Epps *et al.*⁴⁰, allowed control of the organosilane deposition profile by using a specific setup that confined the diffusion to a small gap (≈ 1.5 mm) above the substrate surface, and also by the controlled size and position of the reservoir.

To verify the linear concentration profiles of the functionalized substrates, static contact angle measurements were used. The data was collected at five equidistant points on the surface at 5 mm intervals. The one-dimensional gradient formation was identified by the gradually changing contact angle across the surface of the chlorine, azide, amine and hydroxyl terminated gradients (Figure 4.1). The contact angle increased along the

length of the gradients and the gradual change of the surface energy is noted by the variation of concentrations. The standard uncertainty of contact angle measurements at each position was determined by the standard error between independent measurements on three samples prepared under identical conditions.

For the chlorine FCGS, the water contact angle increased from $39\pm 2^\circ$ to $64\pm 2^\circ$ across the gradient. After the S_N2 substitution of chlorine end group by azide, the contact angle of the gradient decreased, varying from $28\pm 2^\circ$ to $50\pm 1^\circ$. For the amine FCGS, after the phosphanimine hydrolization of the azide FCGS, the contact angles went from $38\pm 1^\circ$ to $56\pm 1^\circ$. Finally, after the alkyne-azide cycloaddition, for the hydroxyl FCGS, the contact angles ranged from $20\pm 1^\circ$ to $43\pm 2^\circ$. These changes were due the different hydrophobicity of each functional group, and indicated that all reactions were successfully completed.

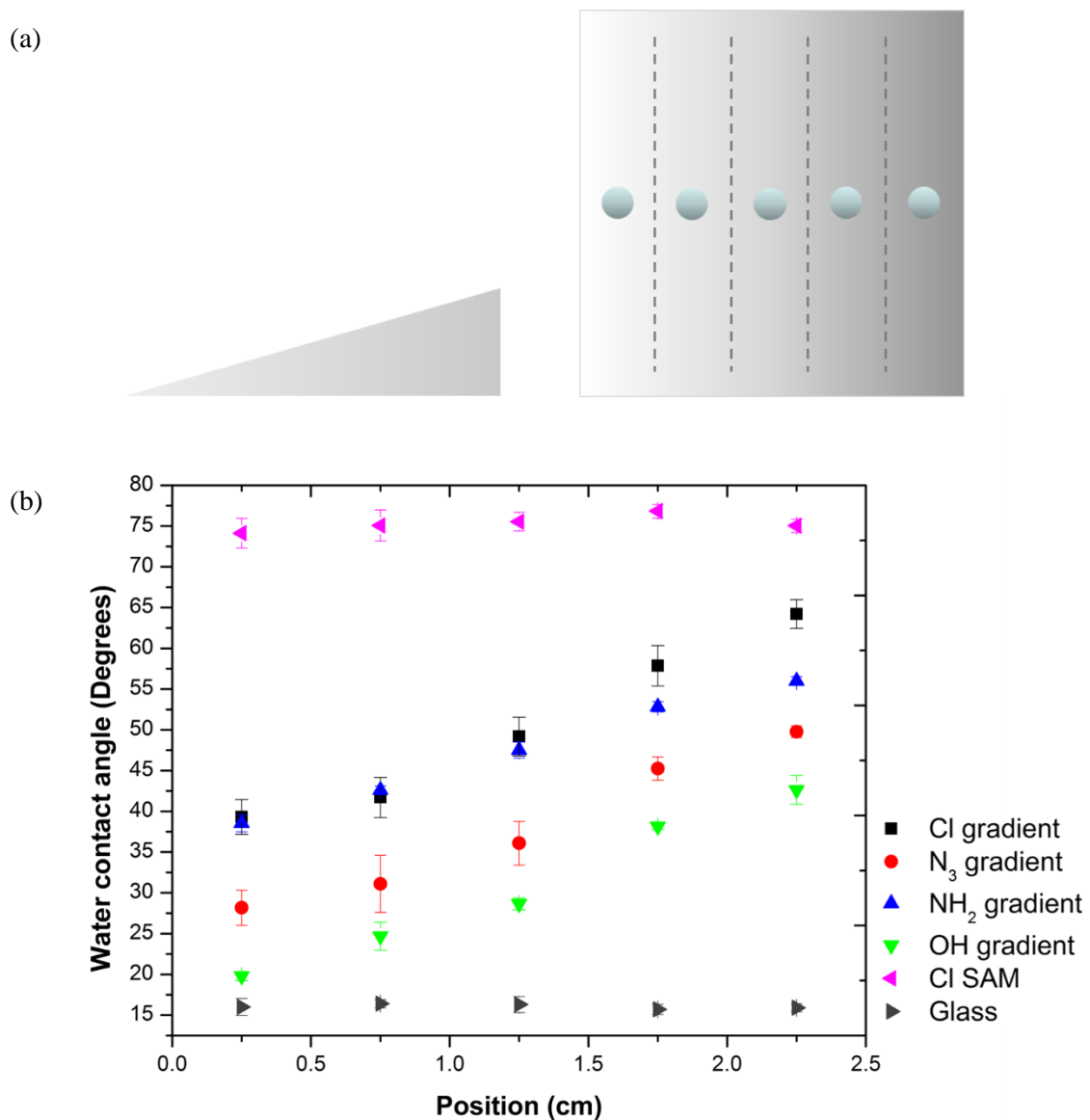


Figure 4.1: (a) Scheme of contact angle points distribution across the substrates. The data was collected from five equidistant points on the surface at 5 mm intervals. (b) Gradient concentration profiles for chlorine (Cl), azide (N₃), amine (NH₂) and hydroxyl (OH) FCGS, and for chlorine uniform SAM and clean glass slide, measured by water contact angle. Static contact angle changed gradually across the surface of the FCGS as reflect of the increasing of the organosilane concentration. Changes in contact angle between terminal group substrates indicated that reactions were successfully completed. Deionized water static contact angle (mean \pm S.E., n = 3).

4.1.2 X-ray Photoelectron Spectroscopy

Previous studies have reported that terminal chemical groups could, for example, control cell growth and modulate cell adhesion to the substrate. Therefore, the response of chondrocyte cells to two different chemical groups, amine (-NH₂) and hydroxyl (-OH) was investigated. The functionality of each engineered substrate was verified using X-ray photoelectron spectroscopy (XPS) survey spectra (0-700 eV), by identification of the monolayer components.

In the survey spectra for the chlorine functionalized substrate, it was observed that the expected peaks from oxygen (O_{1s}), silicon (Si_{2s} and Si_{2p}) and carbon (C_{1s}) were present. One additional peak at 201 eV corresponding to the chlorine (Cl_{2p}) was also present, from where it was assumed that 4-chlorobutyldimethylchlorosilane was successfully grafted onto the surface (Figure 4.2).

In the survey spectra for the amine functionalized substrate, the loss of the Cl_{2p} signal was observed, which indicated that the S_N2 substitution of the chlorine end group by azide group, followed by the phosphanimine hydrolyzation with reduction of the azide terminal group to a primary amine terminal group, was successfully completed (Figure 4.3).

In the survey spectra for the hydroxyl functionalized substrate, besides the loss of the chlorine peak, a small peak around 400 eV, corresponding to nitrogen (N_{1s}) was determined, confirming the efficient alkyne-azide cycloaddition reaction and complete conversion of the chlorine terminal group to hydroxyl terminal group (Figure 4.4).

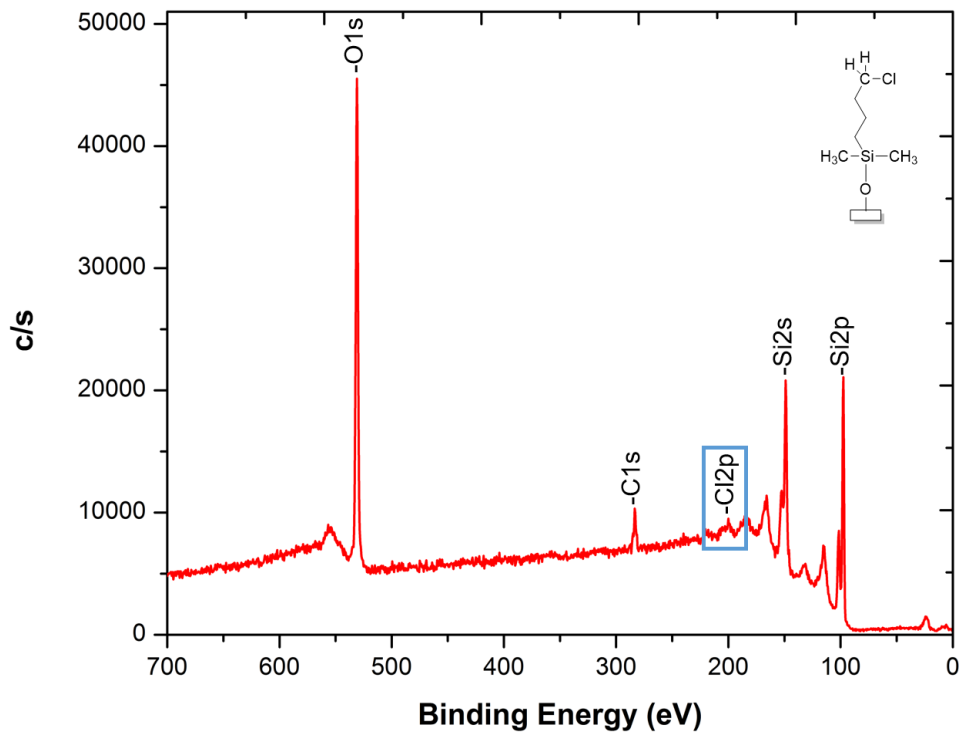


Figure 4.2: Survey spectra (0-700 eV) from XPS for the chlorine surface concentration gradient. The peak at 201 eV, assigned as Cl_{2p}, verified that the chlorine was successfully tethered onto the silica wafer surface.

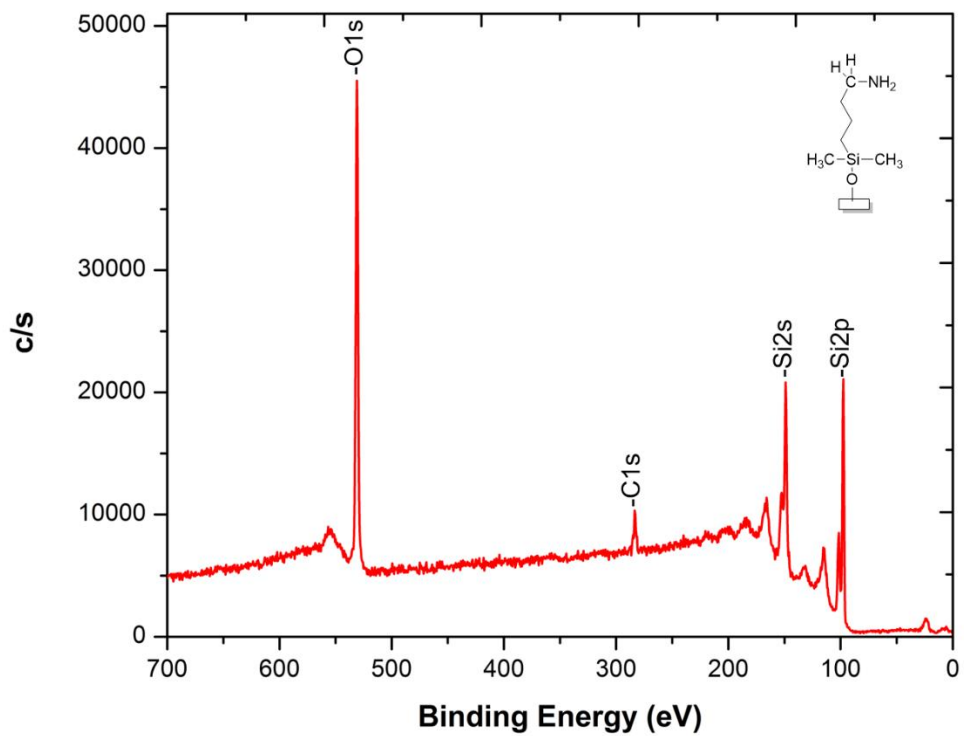


Figure 4.3: Survey spectra (0-700 eV) from XPS for the amine surface concentration gradient. The peak at 201 eV, assigned as Cl_{2p} , disappears, which indicates that the chlorine was quantitatively converted to amine functionality.

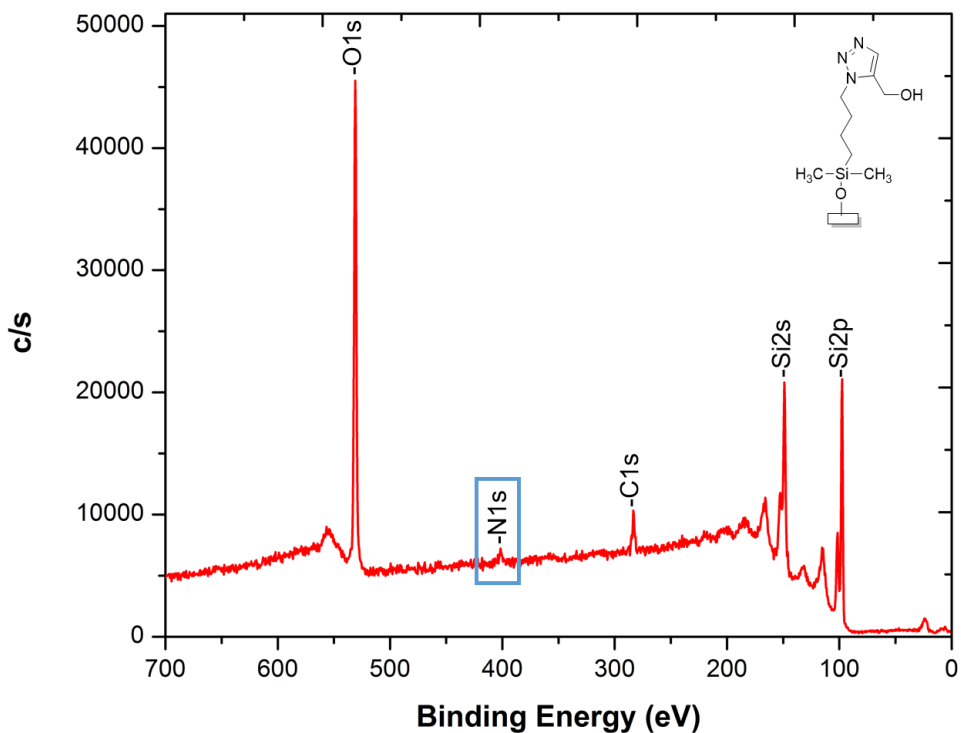


Figure 4.4: Survey spectra (0-700 eV) from XPS for the hydroxyl surface concentration gradient. The peak at 201 eV, assigned as Cl_{2p}, disappears, and a new peak evolves at 400 eV, assigned as N_{1s}. It could be inferred that the chlorine functionalized surface was quantitatively converted to a hydroxyl functionalized surface.

The concentration profile was also verified using high resolution C_{1s} spectra for the chlorine FCGS (Figure 4.5). The C_{1s} curves were fit based on Gauss-Lorentz function with Multipak software, considering a linear background, and peak areas were calculated by integration as described previously. The peak area increased along the gradient position, which confirmed the results obtained by contact angle measurements.

After decomposition of the C_{1s} peak, it showed to consist of two components, one at 284.8 eV related to C-C and C-H groups, and one at 286.5 eV related to C-Cl group.⁴⁵ The overall peak area was analyzed with Multipak and the surface coverage fraction calculated by dividing the overall area under the peak by the number of carbons per molecule, by the overall area of a standard sample peak by the number of carbons per molecule of the standard sample, as shown in equation 4.1:

$$\text{surface coverage fraction} = \frac{\frac{\text{Area}_{\text{peak}}}{\text{number of carbons of sample}}}{\frac{\text{Area}_{\text{peak},0}}{\text{number of carbons of standard sample}}} \quad \text{Equation 4.1}$$

The standard sample was prepared and tested under similar conditions as our samples.

With the surface coverage fraction, the surface concentration was calculated by equation 4.2:

$$\text{surface concentration} = \text{coverage fraction} \times \text{concentration of 100\% coverage}$$

$$\text{Equation 4.2}$$

The concentration of 100% coverage was considered as a silane deposition density of 465 pmol/cm².⁴⁶ The surface coverage fraction and surface concentration were plotted versus the gradient position (Figure 4.6). It was assumed total conversion of chlorine end group to amine and hydroxyl end groups after the respective reactions. The surface

concentration of uniform SAMs was calculated by extrapolation of the calibration curve, and found to be 240 pmol/cm².

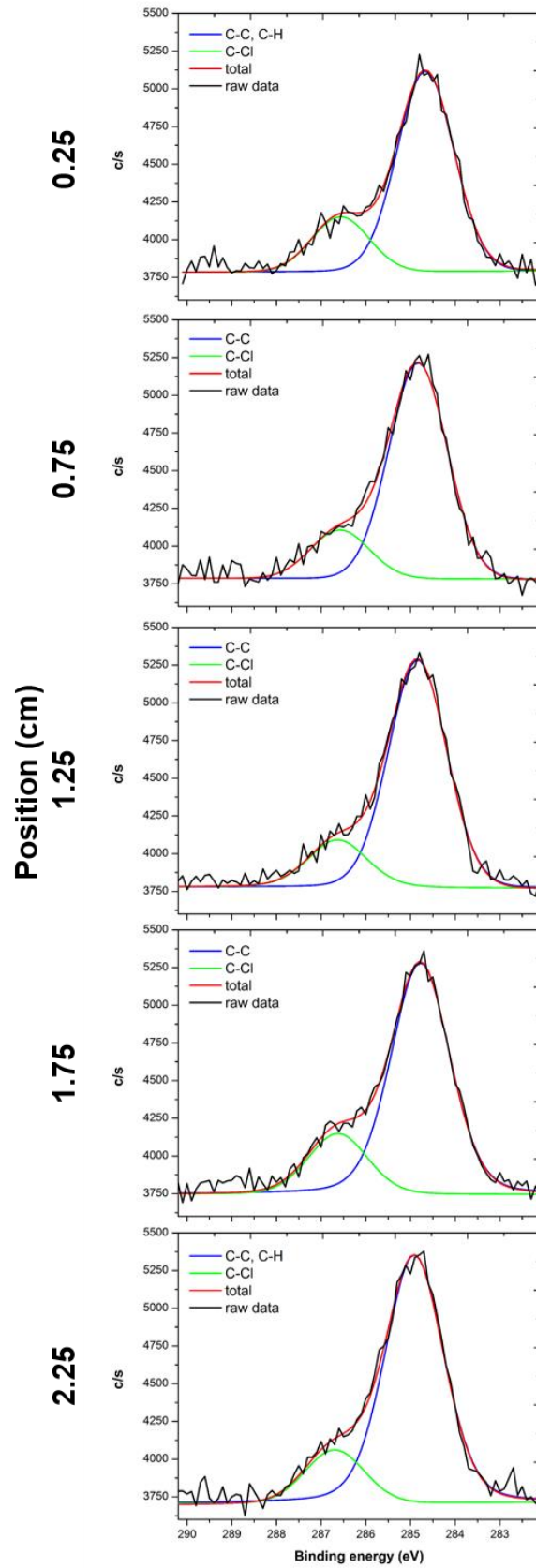


Figure 4.5: Peak fitting of XPS C_{1s} high resolution spectra for each gradient position on chlorine FCGS. The peak area increased along the substrate position, which implied that the concentration increased along the gradient. Decomposition was based on Gauss-Lorentz function.

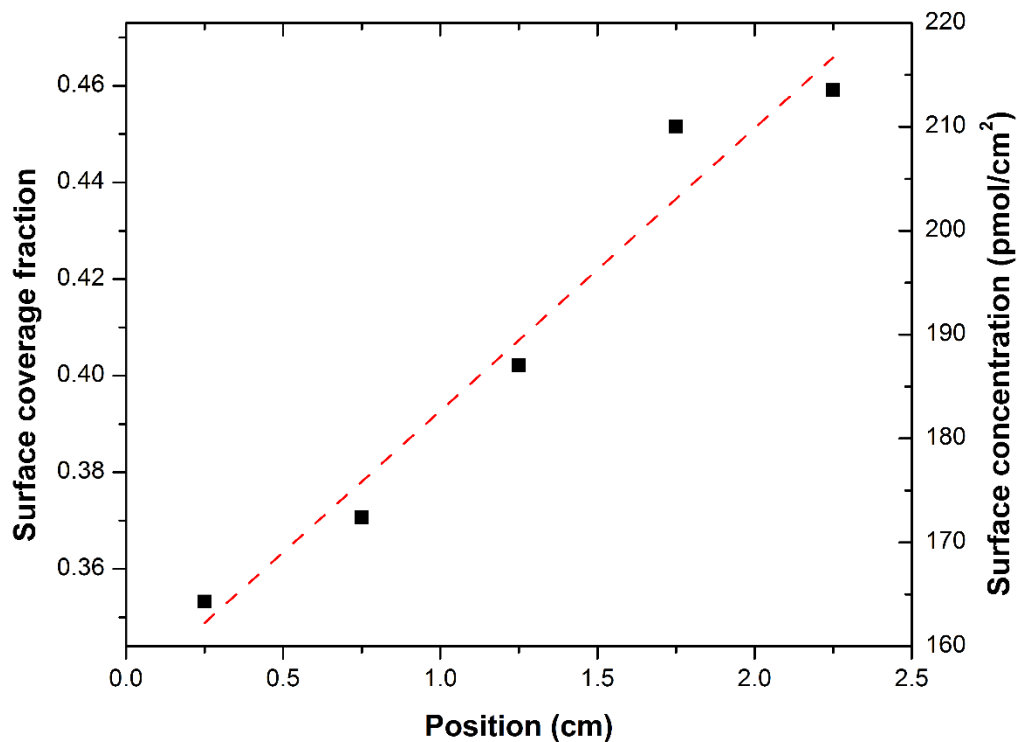


Figure 4.6: Surface concentration and surface coverage fraction as a function of position along the chlorine-terminated gradient surface, determined by XPS ($n = 3$).

4.2 *In vitro* study

The amine and hydroxyl FCGS systems were used to correlate primary human osteoarthritic chondrocyte proliferation and phenotype maintenance by cell number counting and chondrogenic phenotype CD14/CD90 ratios.

4.2.1 Proliferation assay

In order to study the chondrocyte density and proliferation as a function of hydroxyl and amine functionalized gradient concentrations, the samples were stained for cell nuclei (DAPI, blue) after 1, 3 and 7 days of culture. The number of cells at each gradient position was quantified via nuclear staining counts, and the number of cells per area was plotted as a function of FCGS position.

Statistical testing showed that differences in cell proliferation for both hydroxyl and amine functionalized substrates were significant. Furthermore, one-way analysis of variance (ANOVA) was performed to analyze the data, comparing same positions of the gradients in different time points, and different positions of the gradient in a same time point.

For the hydroxyl terminated FCGS, after 24 hours of culture (day 1), the number of adherent cells was higher (18 ± 4 cells/mm²) at the lower concentration, around 162 pmol/cm² (position 0.25 mm), decreasing along the gradient and reaching a second peak at 201 pmol/cm² (16 ± 2 cells/mm²). At positions 0.25 mm and 0.75 mm, corresponding to 162 pmol/cm² and 175 pmol/cm², it was observed that the number of cells decreased over 3 d and 7 d of culture, while in positions 1.25 mm and 1.75 mm (surface concentration from 188 pmol/cm² to 201 pmol/cm²) the number of cells initially decreased (3 d) and

increased again (7 d). Overall, it was assumed that the position 1.75 mm of the hydroxyl gradient could indicate the best hydroxyl surface concentration for the chondrocyte cells proliferation, 201 pmol/cm² (Figure 4.7).

For the uniform hydroxyl functionalized SAM substrates, which possessed a concentration of 240 pmol/cm², it was observed a higher number of cell adherence at 1 d when compared to any position of the hydroxyl gradient. We see a general decrease of cell number over time, and the count at 7 d was characterized by a more uniform cell distribution response, considering the more constant cell distribution over the substrate (Figure 4.8).

For the amine terminated FCGS, the cell adhesion at all the positions was suitable, since chondrocytes were seeded at 30 cell/mm² and the adhesion fluctuated from 28 ± 2 cell/mm² at 188 pmol/cm² to 31 ± 3 cell/mm², after 24 hours of culture. However, the cell number decreased at all positions along the time (after 3 d and 7 d of culture). After 7 d of culture, the cell number was higher at lower concentrations of the gradient, with a mean of 19 ± 1 cells/cm² at position 0.25 mm of the substrate, corresponding to 162 pmol/cm² (Figure 4.9).

For the amine functionalized SAM substrates, at a uniform concentration of 240 pmol/cm², the same phenomena of cell adhesion was observed after 24 hours, followed by a decrease in cell number after 3 d and 7 d of culture. The fluctuations of cell distribution along the substrate were more discrete than for the amine gradient substrates (Figure 4.10).

Overall, chondrocyte cells adhered and proliferated significantly higher on amine functionalized substrates compared to hydroxyl substrates. These results were expected based on previous studies reported in literature, where self-assembled monolayers of

organosilanes have been used to evaluate the effect of surface chemistry on cell behavior for different cell lines, and the amine group was reported to have a positive effect on cell adhesion, spreading and growth, when compared to other functional groups.⁴⁷⁻⁴⁹

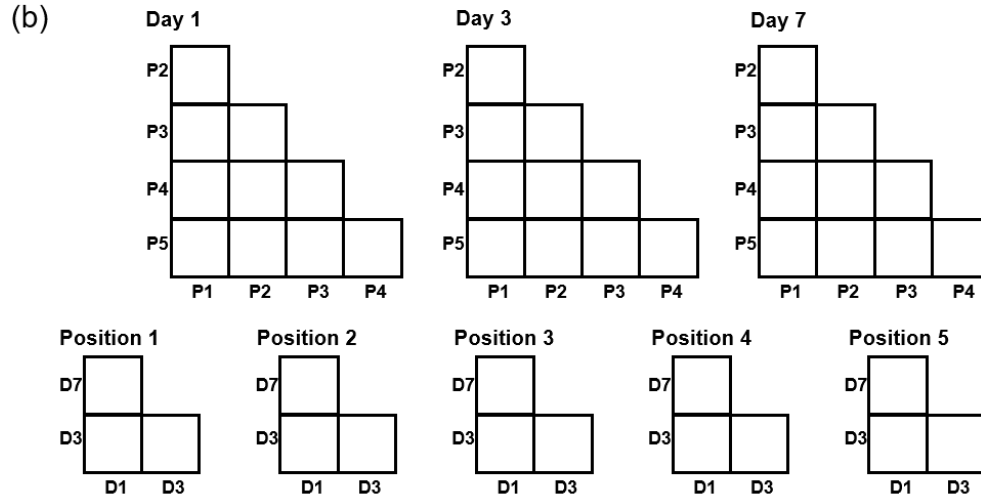
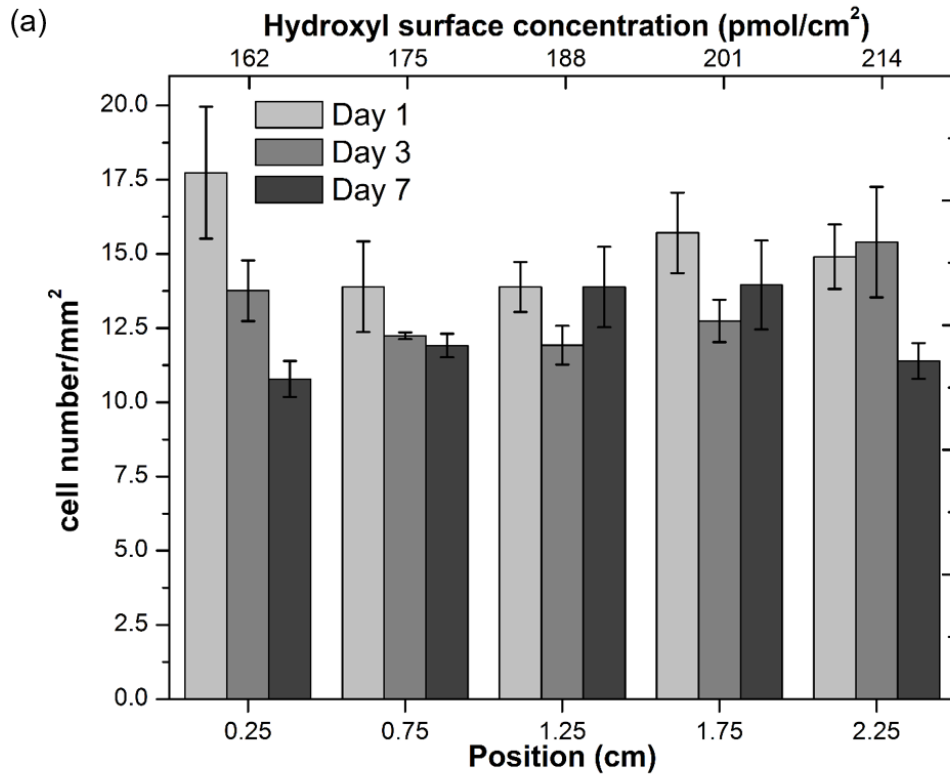


Figure 4.7: (a) Chondrocyte proliferation response as a function of hydroxyl concentration on hydroxyl FCGS. Cell number was collected at each sample position after days 1, 3 and 7 of culture. Values are represented as means \pm standard error (S.E.), with $P < 0.05$ and $n = 3$. (b) Statistical analysis for cell proliferation on hydroxyl gradients data. Grey shaded boxes indicate significant differences for cell number from different positions in a same time point, or different time points in a same position (ANOVA with Tukey's, $P < 0.05$).

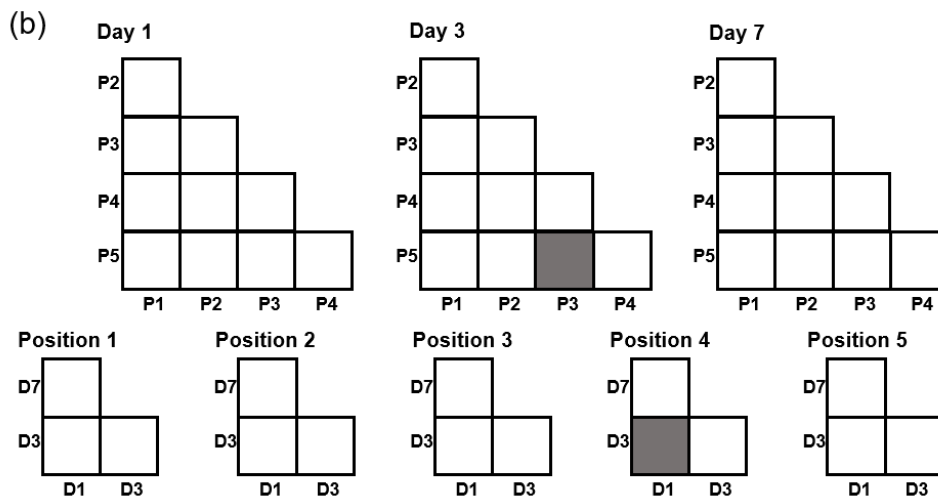
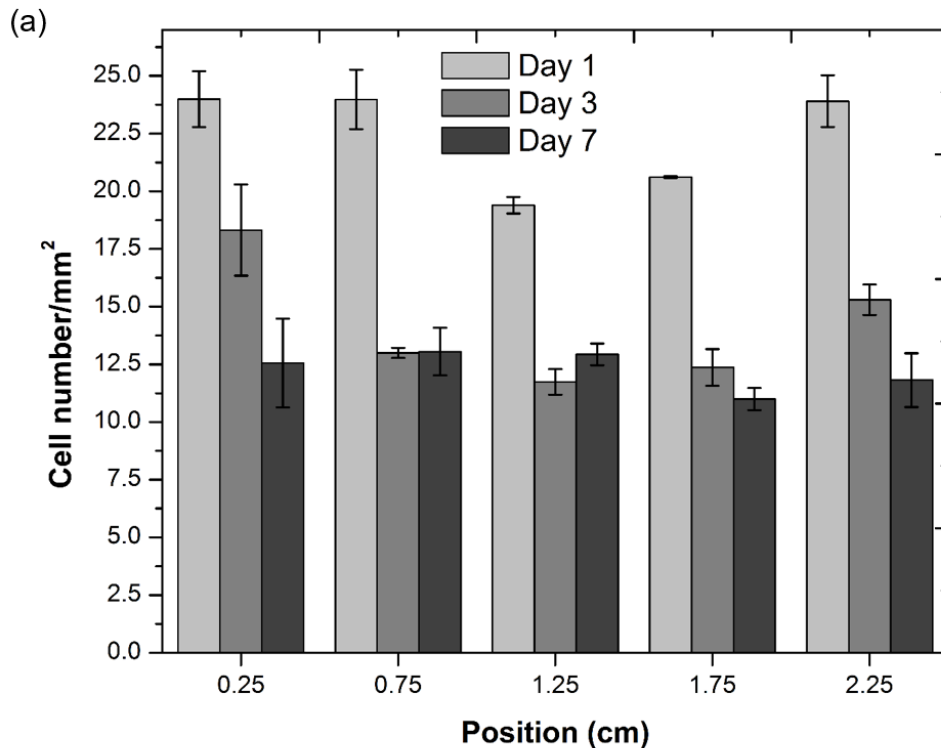


Figure 4.8: (a) Human primary chondrocyte proliferation response in hydroxyl SAM substrate, with uniform concentration of 240 pmol/cm². Cell number was collected at each sample position after days 1, 3 and 7 of culture. Values are represented as means \pm S.E., with $P < 0.05$ and $n = 3$. (b) Statistical analysis for cell proliferation on hydroxyl uniform SAM data. Grey shaded boxes indicate significant differences for cell number from different positions in a same time point, or different time points in a same position (ANOVA with Tukey's, $P < 0.05$).

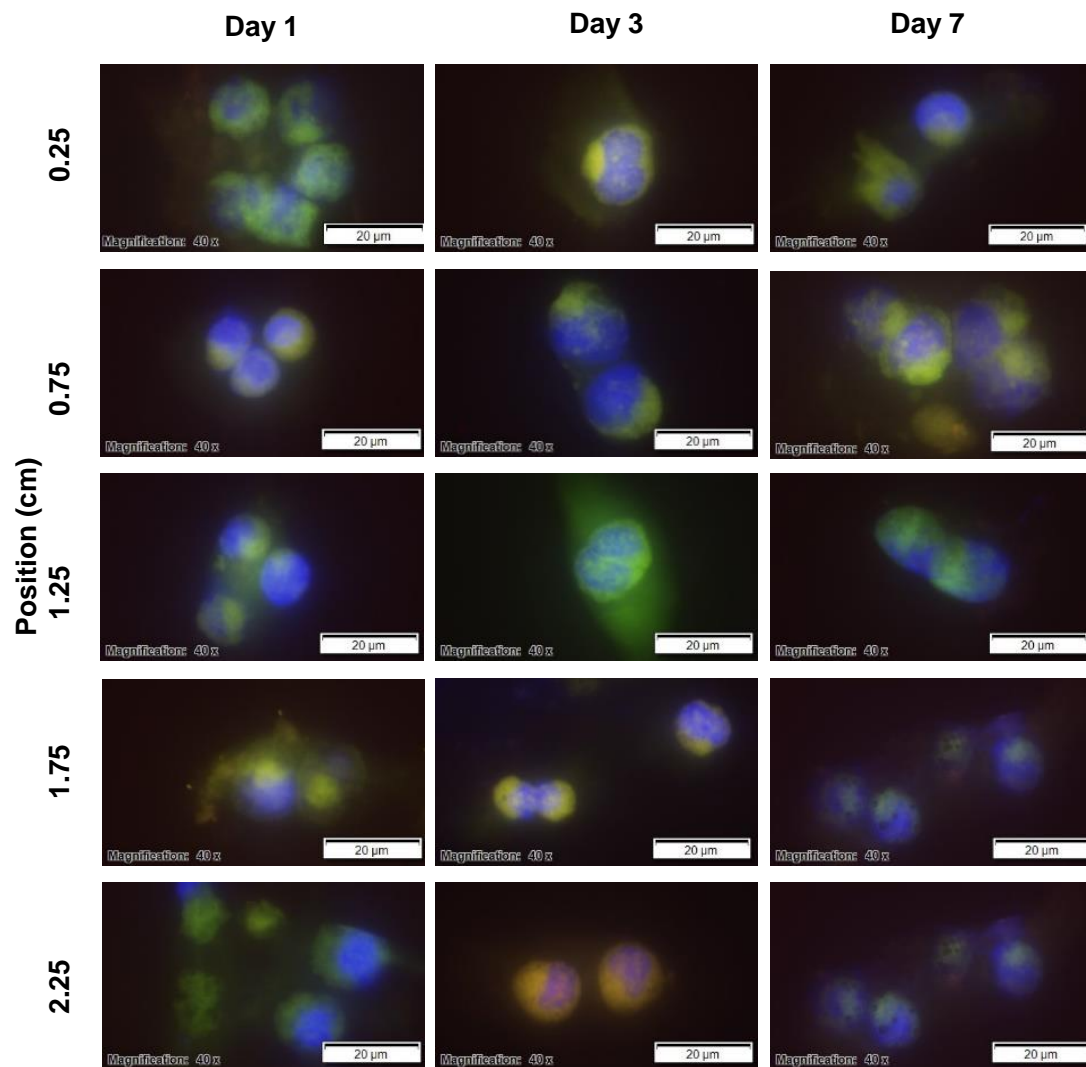


Figure 4.9: Immunofluorescent staining of actin (red), C5-maleimide (green) and nuclei (blue) for human primary chondrocyte culture on hydroxyl functionalized gradient surface after days 1, 3 and 7 of culture. Images were taken every 5 mm down length of the gradient. Scale bar = 20 μm .

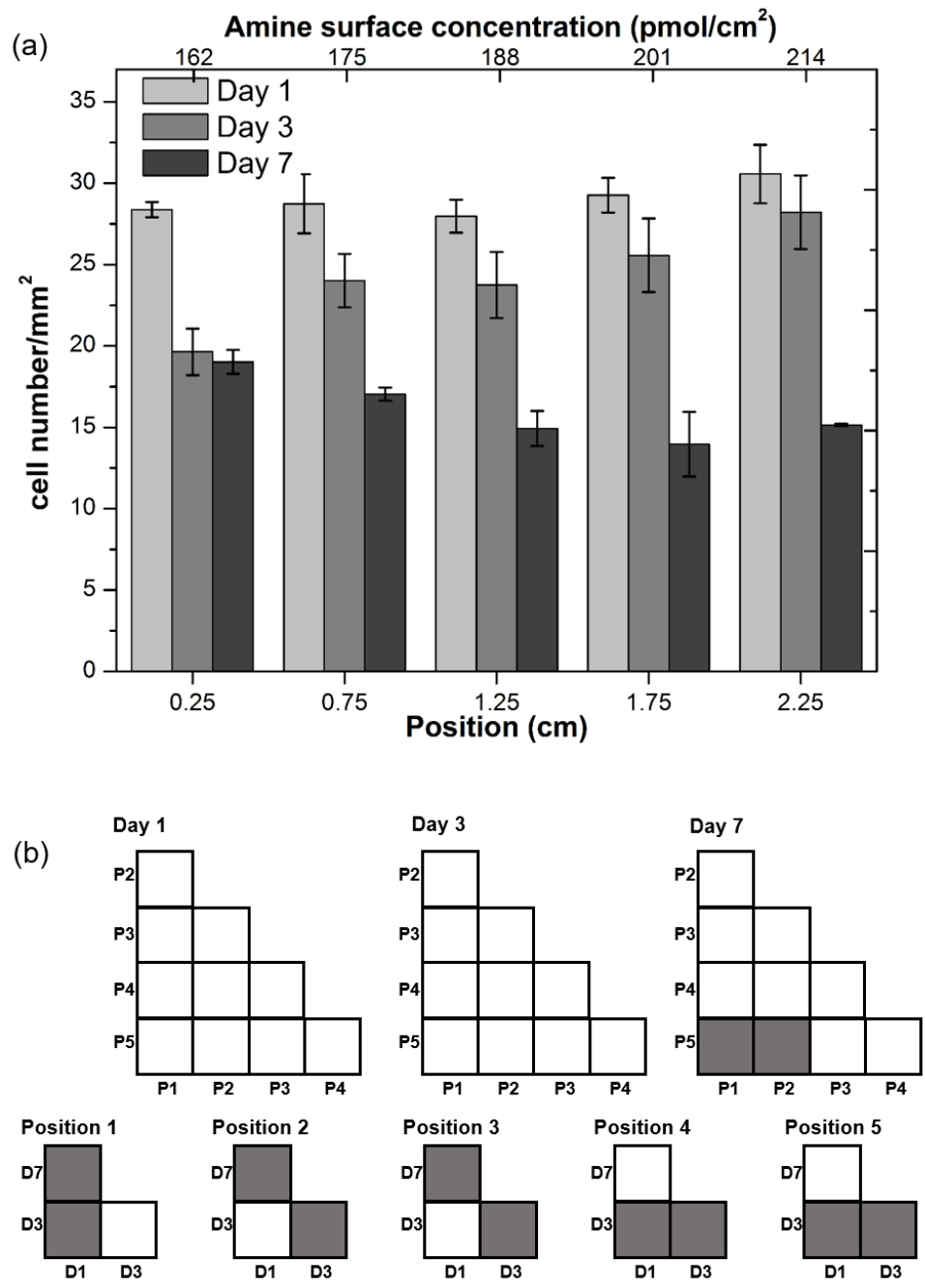


Figure 4.10: (a) Human primary chondrocyte proliferation response as a function of amine concentration on functionalized amine FCGS. Cell number was collected at each sample position after days 1, 3 and 7 of culture. Values are represented as means \pm S.E., with $P < 0.05$ and $n = 3$. (b) Statistical analysis for cell proliferation on amine gradients data. Grey shaded boxes indicate significant differences for cell number from different positions in a same time point, or different time points in a same position (ANOVA with Tukey's, $P < 0.05$).

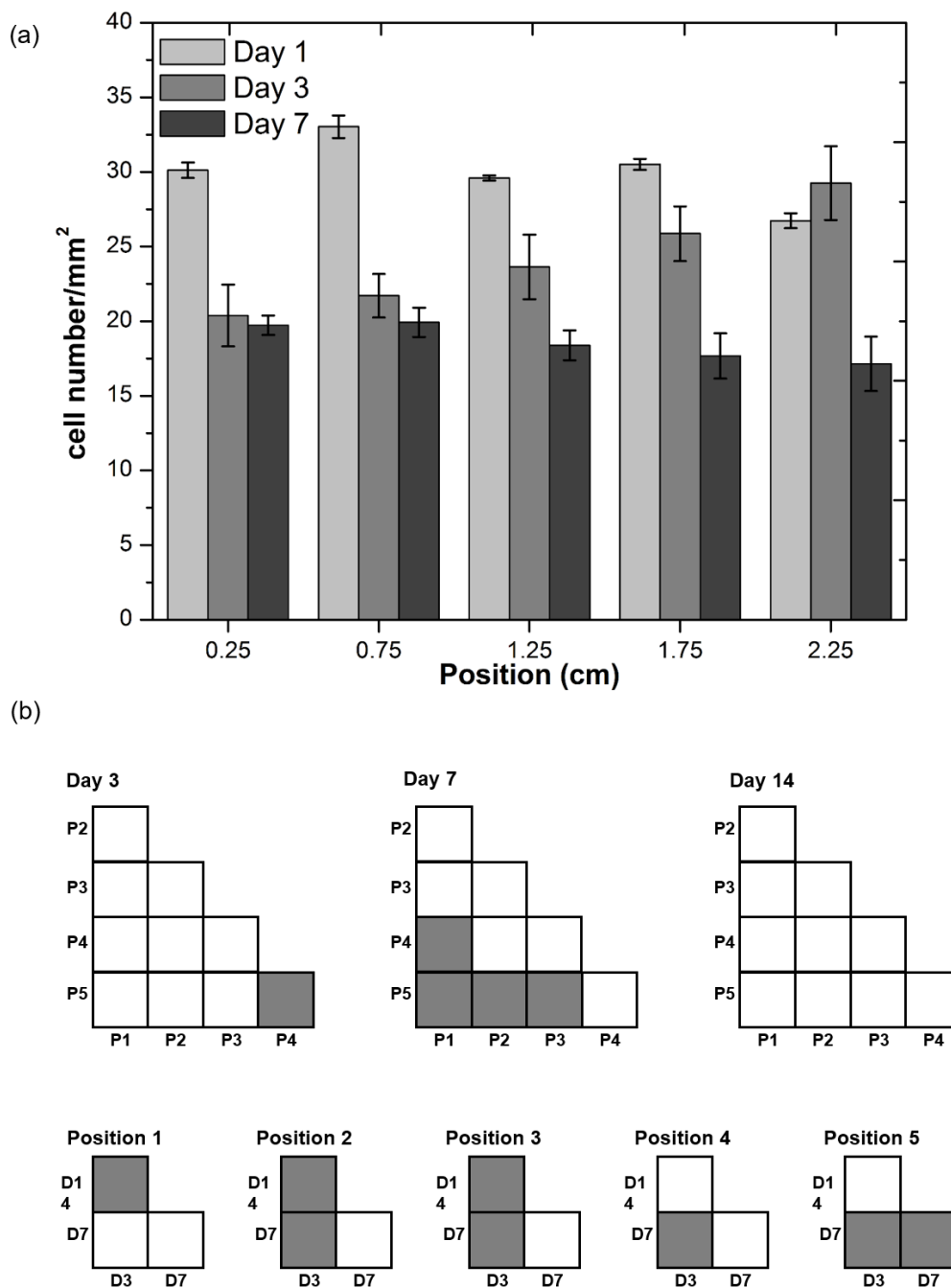


Figure 4.11 (a) Human primary chondrocyte proliferation response in amine SAM substrate, with uniform concentration of 240 pmol/cm². Cell number was collected at each sample position after days 1, 3 and 7 of culture. Values are represented as means \pm S.E., with $P < 0.05$ and $n = 3$. (b) Statistical analysis for cell proliferation on amine gradients data. Grey shaded boxes indicate significant differences for cell number from different positions in a same time point, or different time points in a same position (ANOVA with Tukey's, $P < 0.05$).

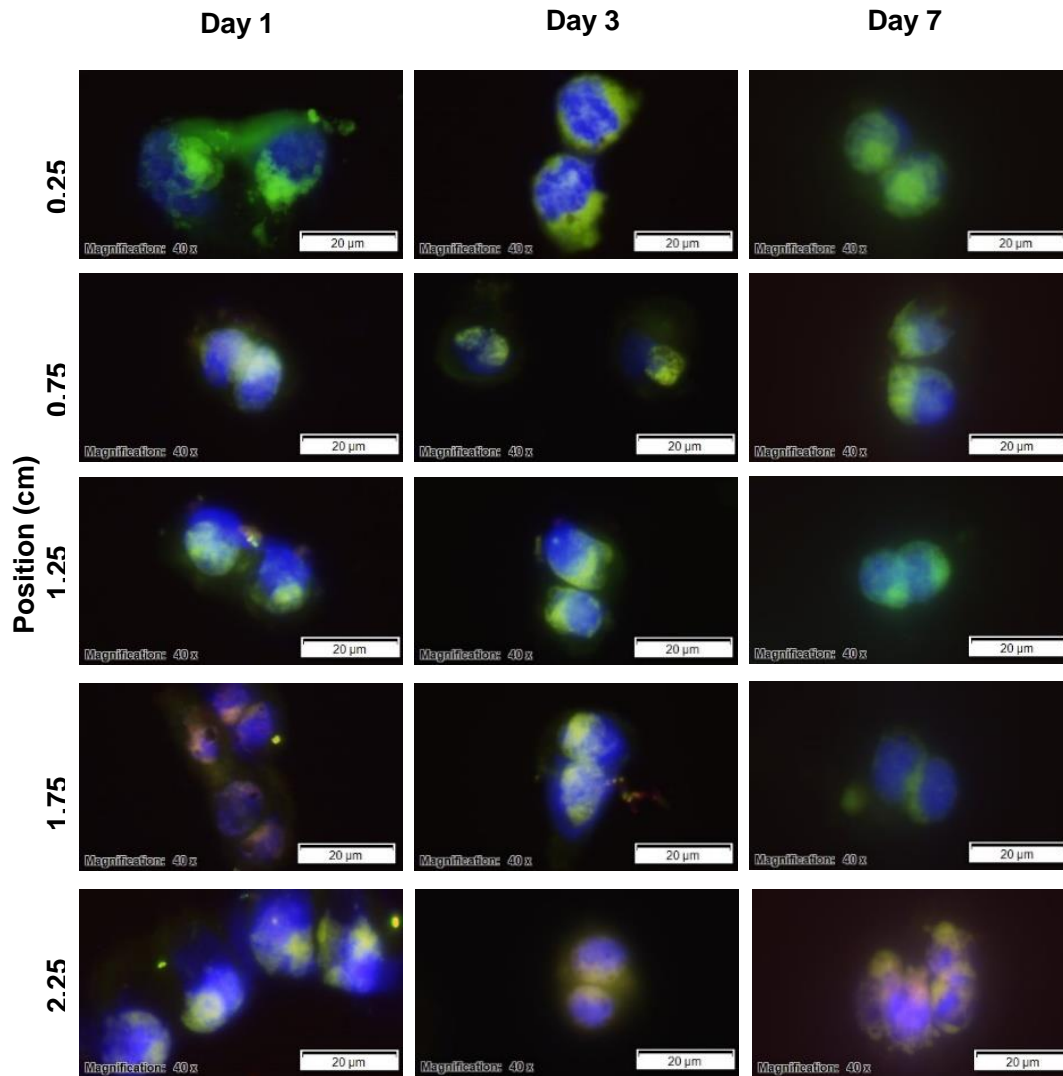


Figure 4.12: Immunofluorescent staining of actin (red), C5-maleimide (green) and nuclei (blue) for human primary chondrocyte culture on amine functionalized gradient surface after days 1, 3 and 7 of culture. Images were taken every 5 mm down length of the gradient. Scale bar = 20 μm .

Actin organization was also observed over the 1 d, 3 d and 7 d of culture (Figures 4.9 and 4.12). Different surface functionalization has been shown to influence the chondrocyte shape and modulate the cytoskeletal arrangement, which can alter the cellular behavior.⁴² Differentiated chondrocytes have a characteristic rounded phenotype with a diffuse actin microfilament network that influence the secretion of ECM components (collagen type II and aggrecan). When attached to a two dimensional substrate, the cells dedifferentiate towards a more fibroblastic phenotype, reorganizing the actin filamentous into distinct stress fibers and adjusting to a spread morphology.⁵⁰ Cellular actin distribution was detected by binding to a red fluorescent labelled phalloidin (excitation/emission: 540/565 nm). It was observed that for both amine and hydroxyl functionalized substrates, at low concentrations of the gradients (162 to 175 pmol/cm²), the chondrocytes retained their rounded morphology shape, and the actin organization tended to be more localized towards one side of the cell, reminiscent of the apical organization of actin in healthy chondrocytes. However, for more concentrated regions (188 to 201 pmol/cm²), it could be visualized that tiny differences in the cytoskeletal organization, appeared to be less organized, similar to previous reports of OA chondrocytes.⁴² This difference became more pronounced after 7 days of culture. The actin filaments were also decorated with tropomyosin labeled with Alexa fluor 488 C5 maleimide (green) ⁵¹, and the superposition of the green and red fluorescence confirmed the observed results for cytoskeletal organization.

4.2.2 Phenotype maintenance assay

In order to quantify chondrocyte phenotype maintenance as a response of each engineered FCGS position, the two surface markers CD14 and CD90 were used. The

surface marker CD14 is a lipopolysaccharide receptor found on freshly isolated chondrocytes, while the surface marker CD90 is a glycosylphosphatidylinositol-anchored glycoprotein associated with cellular proliferation.⁴²

As introduced before, when human articular chondrocytes are cultured *in vitro*, they undergo the phenomenon of dedifferentiation. These cells change the production of ECM components as well as surface markers. At the same time there is a down regulation of collagen type II, aggrecan and the surface marker CD14, whilst there is an up regulation of collagen type I, versican and CD90. Usually, the ratios Col2/Col1 and aggrecan/versican are used as traditional phenotype indicators, but Diaz-Romero *et al.* (2008) have reported a similar pattern for the ratio CD14/CD90, with the advantage of a faster decreasing of the ratio with time, which indicates that CD14/CD90 can be used as a membrane based chondrocyte differentiation index.⁵² In a similar study, Giovannini *et al.* (2010) studied changes at the protein level of different surface markers and ECM components for chondrocyte cells cultured *in vitro*. Their previous results were confirmed at a mRNA gene level and established the CD14/CD90 ratio potential as chondrocyte differentiation index.⁵³

Statistical testing showed that differences in phenotype maintenance based on CD14/CD90 ratio were significant for both hydroxyl and amine functionalized substrates. Furthermore, one-way ANOVA was performed to analyze the data, comparing the same positions of the gradients at different time points, and different positions of the gradient at a same time point.

For the hydroxyl terminated substrates, chondrocytes experienced a decrease in the ratio CD14/CD90 from 3 d of culture to 7 d, and that number increased significantly at day 14 (Figures 4.13 and 4.14). For the FCGS substrates, the CD14/CD90 ratio had similar

pattern in intermediate concentrations from 175 to 201 pmol/cm² (positions 0.75 mm to 1.75 mm), but an extremely high number at position 2.25 mm (higher concentration), corresponding to 214 pmol/cm². The same trend was observed for the uniform SAM hydroxyl surface, and it could be associated to a border interference. Overall, it was concluded that the hydroxyl functionalized substrates promoted chondrocyte survival after long periods of culture, and the increased ratio CD14/CD90 at 14 d compared to 3 d could be associated the cell proliferation over time. However, no assumptions could be made about the influences of different concentrations on this cell behavior.

For the amine terminated substrates, the ratio CD14/CD90 increased from 3 d to 7 d, and decreased again at 14 d (Figures 16 and 17). Comparing the different positions of the FCGS, it was observed that intermediate positions had the same pattern, where overall the cells maintained their phenotype comparing 3 d to 14 d. At positions close to the edges (position 0.25 mm and 2.25 mm), cells experienced phenotype loss over time, but this was due to the higher ratio of CD14/CD90 in the local area at 3 d compared to other regions of the substrate, and these discrepancies could be related to an edge effect. At 14 d, all positions had relatively similar ratios and overall the amine functionalized substrates promoted chondrocyte phenotype maintenance.

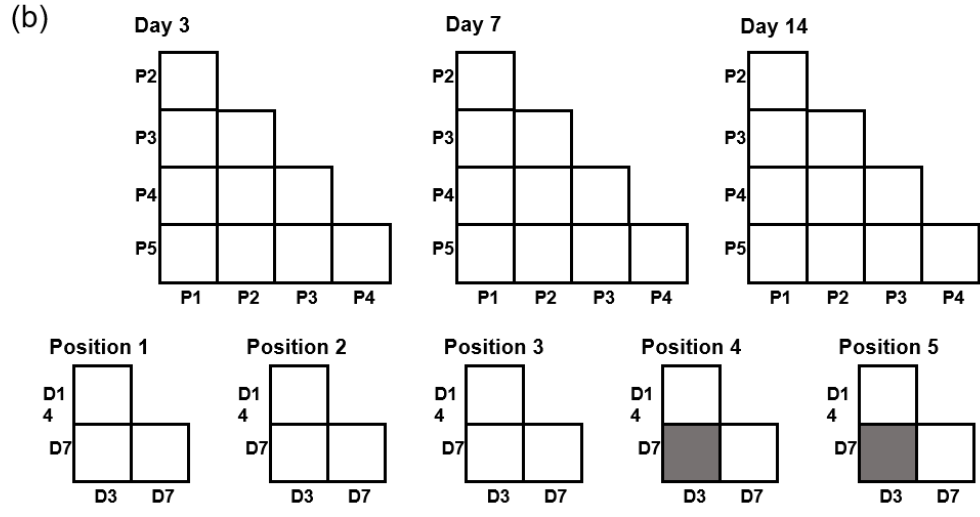
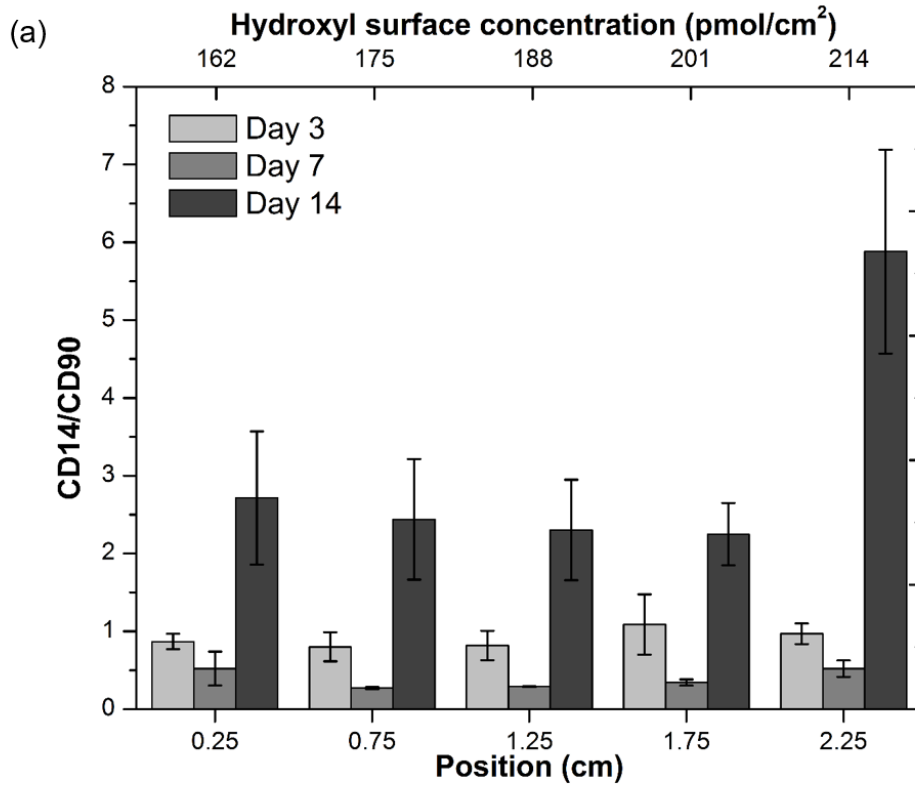


Figure 4.13: (a) Chondrocyte survival of each gradient position based on phenotype maintenance using CD14/CD90 ratios for days 3, 7 and 14 of culture on hydroxyl FCGS. Values are represented as means \pm S.E., with $P < 0.05$ and $n = 3$. (b) Statistical analysis for cell phenotype maintenance on hydroxyl gradients data. Grey shaded boxes indicate significant differences for cell number from different positions in a same time point, or different time points in a same position (ANOVA with Tukey's, $P < 0.05$).

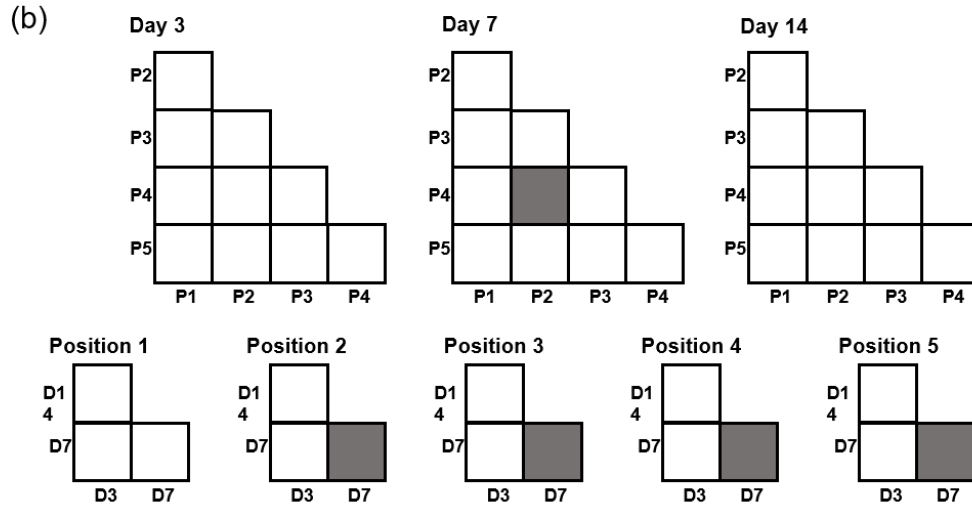
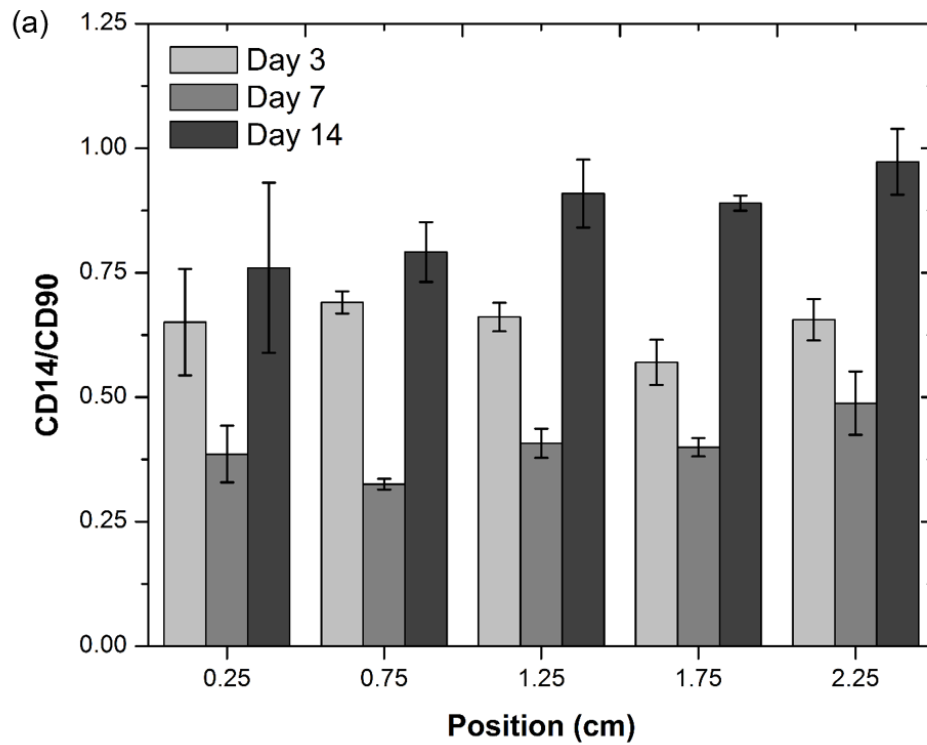


Figure 4.14: (a) Chondrocyte survival of each gradient position based on phenotype maintenance using CD14/CD90 ratios for days 3, 7 and 14 of culture on hydroxyl uniform SAM surface, with uniform concentration of 240 pmol/cm². Values are represented as means \pm S.E., with $P < 0.05$ and $n = 3$. (b) Statistical analysis for cell phenotype maintenance on hydroxyl gradients data. Grey shaded boxes indicate significant differences for cell number from different positions in a same time point, or different time points in a same position (ANOVA with Tukey's, $P < 0.05$).

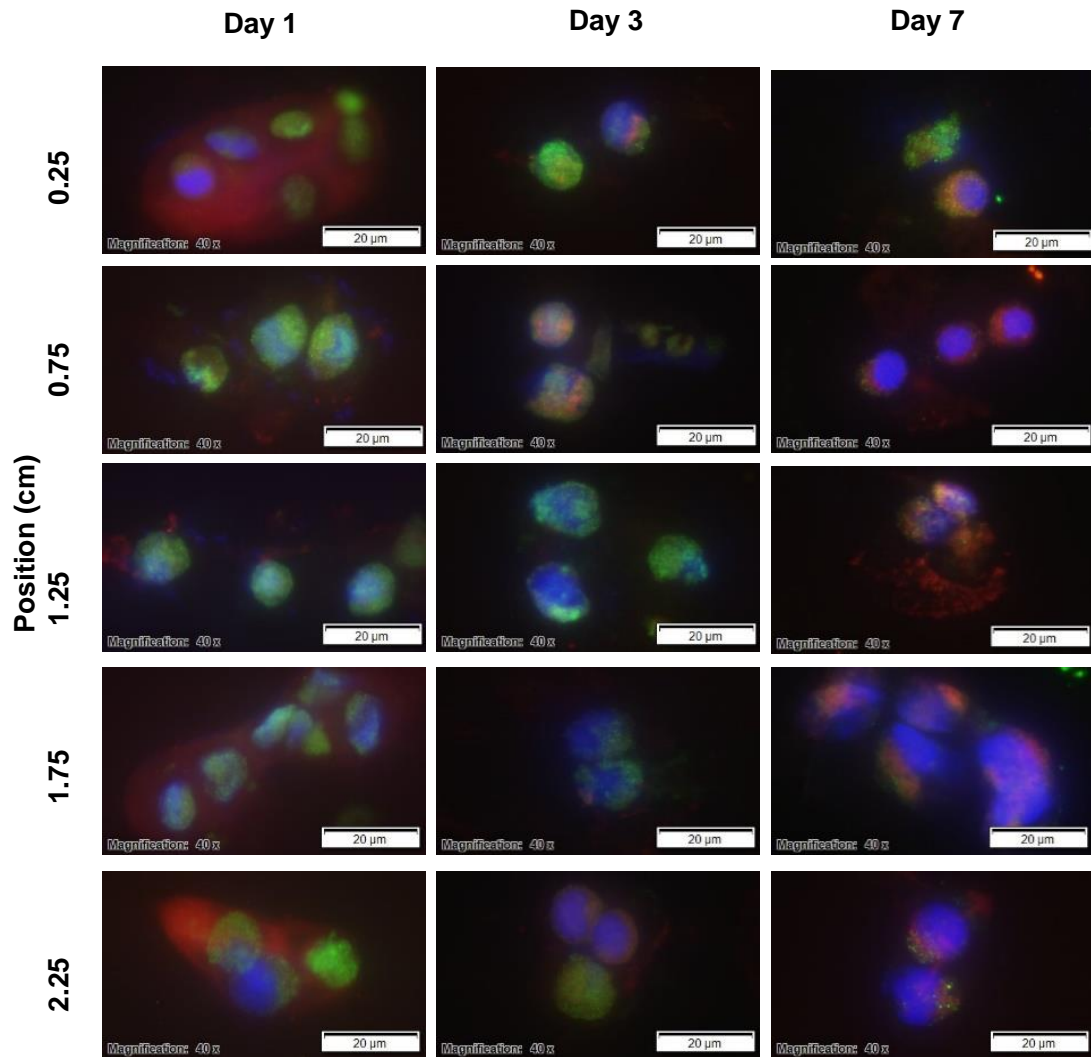


Figure 4.15: Immunofluorescent staining of CD14 (red), CD90 (green) and nuclei (blue) for human primary chondrocyte culture on hydroxyl functionalized gradient surface after days 3, 7 and 14 of culture. Images were taken every 5 mm down length of the gradient. Scale bar = 20 μm .

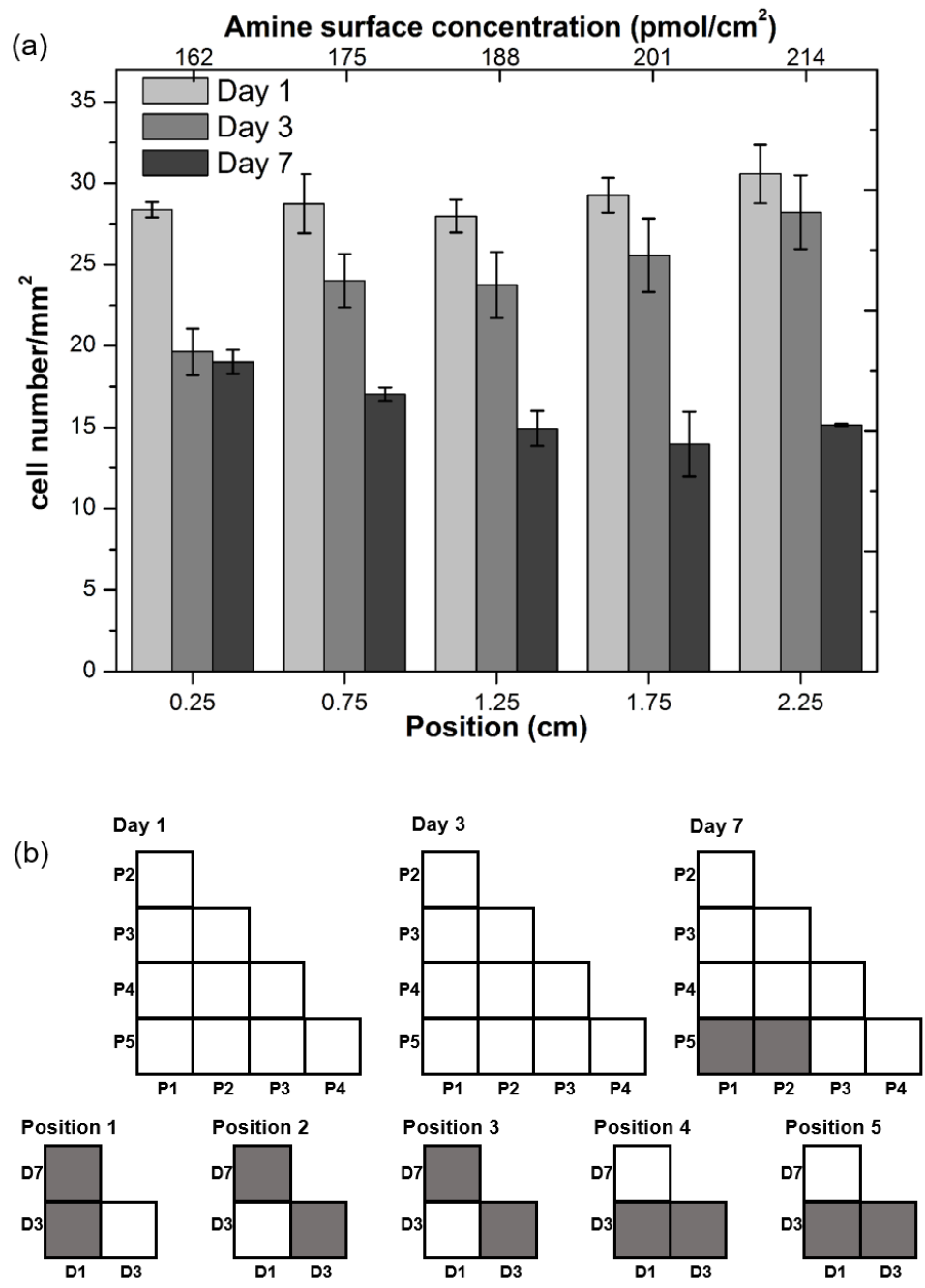


Figure 4.16: (a) Chondrocyte survival of each gradient position based on phenotype maintenance using CD14/CD90 ratios for days 3, 7 and 14 of culture on amine FCGS. Values are represented as means \pm S.E., with $P < 0.05$ and $n = 3$. (b) Statistical analysis for cell phenotype maintenance on amine gradient data. Grey shaded boxes indicate significant differences for cell number from different positions in a same time point, or different time points in a same position (ANOVA with Tukey's, $P < 0.05$).

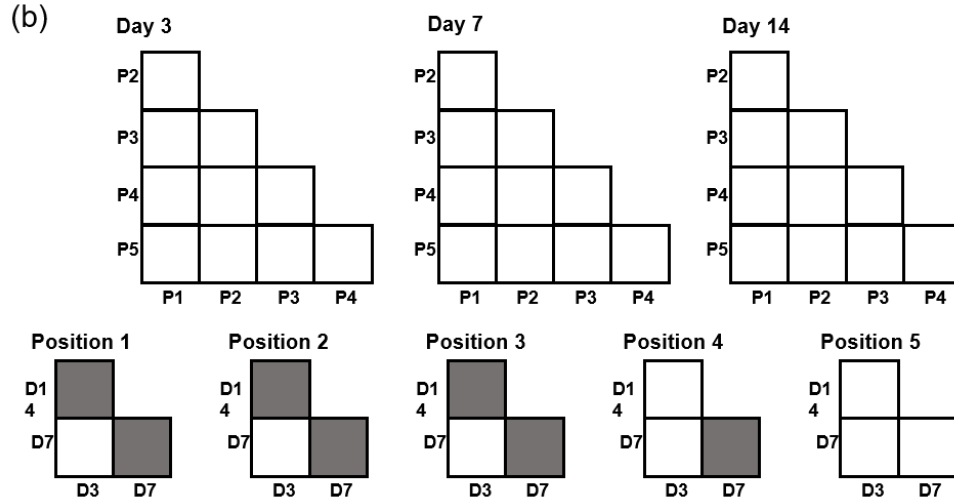
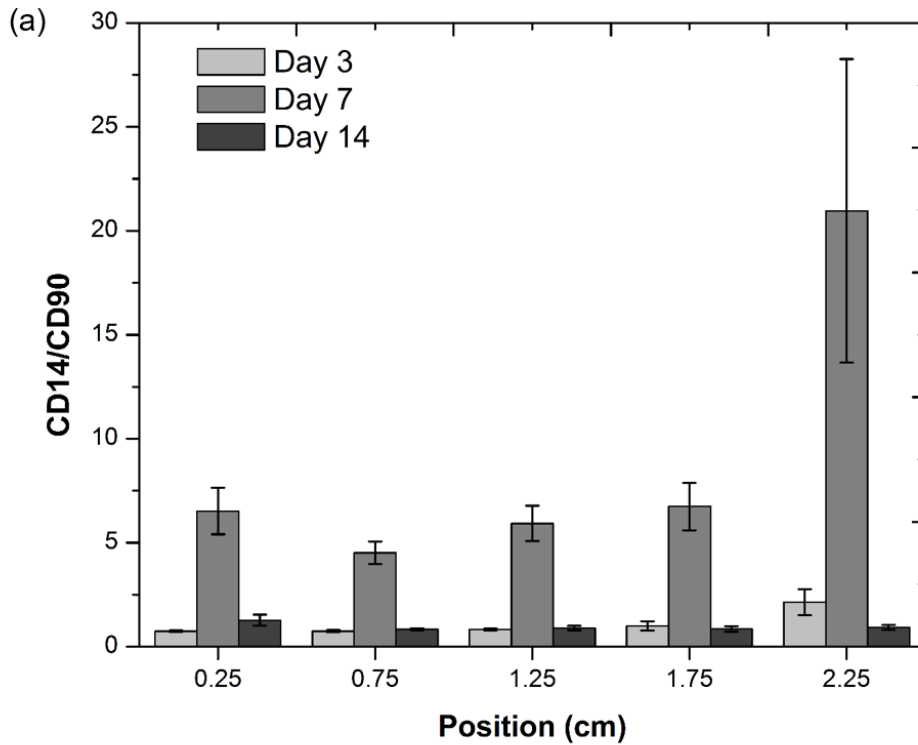


Figure 4.17: (a) Chondrocyte survival of each gradient position based on phenotype maintenance using CD14/CD90 ratios for days 3, 7 and 14 of culture on amine SAM surface, with uniform concentration of 240 pmol/cm². Values are represented as means \pm S.E., with $P < 0.05$ and $n = 3$. (b) Statistical analysis for cell phenotype maintenance on amine uniform SAM data. Grey shaded boxes indicate significant differences for cell number from different positions in a same time point, or different time points in a same position (ANOVA with Tukey's, $P < 0.05$).

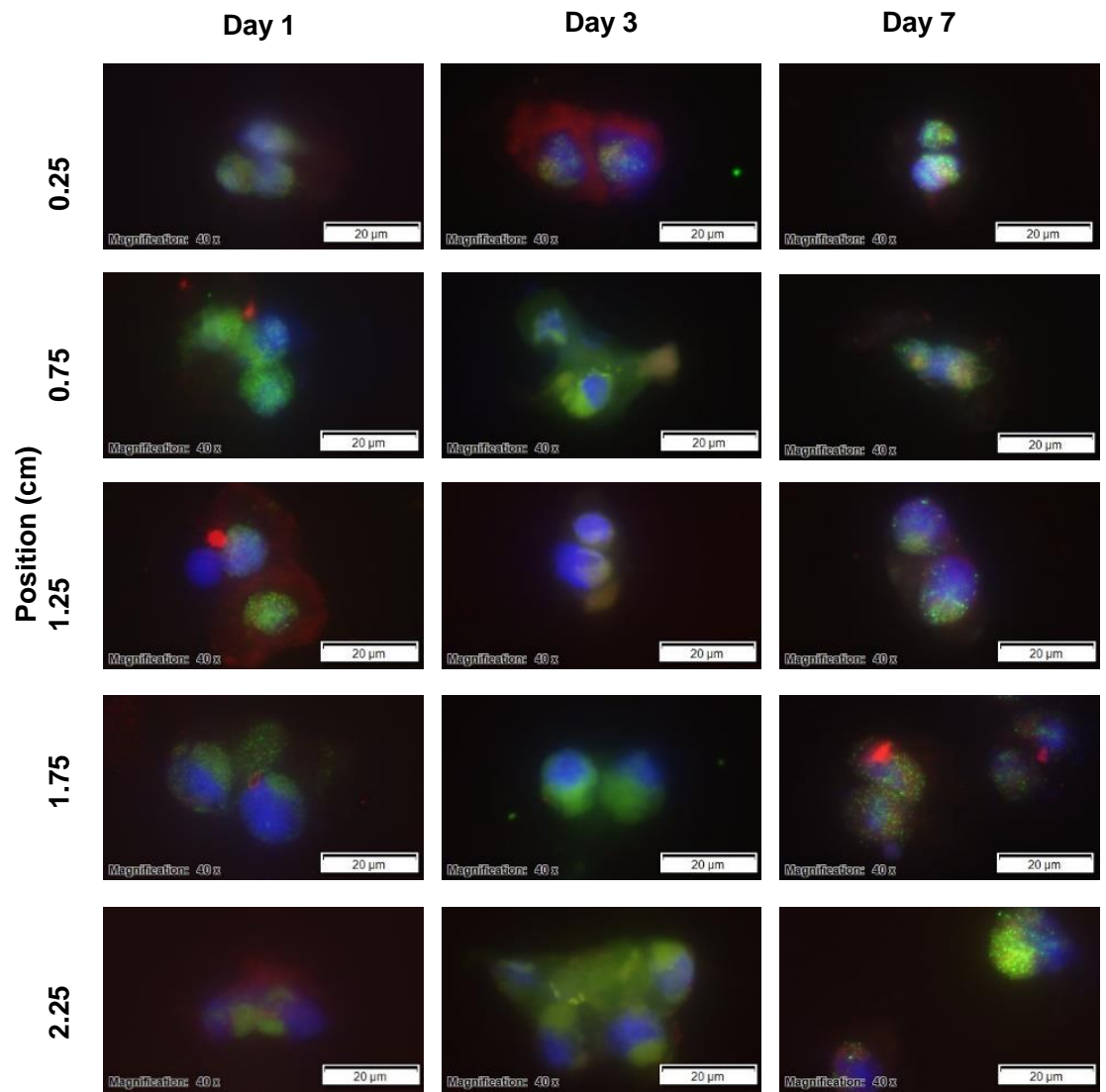


Figure 4.18: Immunofluorescent staining of CD14 (red), CD90 (green) and nuclei (blue) for human primary chondrocyte culture on amine functionalized gradient surface after days 3, 7 and 14 of culture. Images were taken every 5 mm down length of the gradient. Scale bar = 20 μm .

CHAPTER V

CONCLUSIONS

Osteoarthritis (OA) is thought to be the most prevalent dysfunction among the musculoskeletal group disease, specially affecting the population aged 60 years or older. The high prevalence of OA, its social costs and high impact on physical function and quality of life, underline the importance of management of this disorder.⁵⁴ Current treatments include mosaicplasty and microfracture, which can be successful in some aspects to provide short-term pain relief, have limitations and their long term benefits remain elusive. The repaired tissue does not have the same biomechanical properties and eventually breaks down, requiring additional treatments or a total joint arthroplasty.

The cartilage tissue engineering strategies aim to combine reparative cells and porous three-dimensional scaffolds for repairing or restoring the damaged tissue. This scaffold-based therapies require a large number of chondrogenic cells to regenerate the damaged extracellular matrix (ECM) of the articular cartilage, and in order to obtain suitable number of cells, the requirement for extensive *in vitro* expansion in monolayer cultures is apparent. However, during expansion in monolayers, chondrocyte cells lose their phenotype and dedifferentiate, changing the production of ECM components, as well as the physical appearance to that of a fibroblast-like morphology. Therefore, in order to develop a successful cell-based technology for OA treatment, the optimization of the cell expansion process is desired, through regulating the substrate/cell interaction.⁵⁵

The objective of this study was to evaluate whether controlled changes in substrate surface chemistry *via* functionalization with amine and hydroxyl terminated silane could regulate proliferation and phenotype maintenance of primary human chondrocytes, as well as analyze the effects of different concentrations of the terminal chemical groups on chondrocytes behavior.

Substrates were fabricated using a “vacuum away” method which enabled the generation of linear gradient chemical concentration profiles in 25 mm² glass cover slides. The linear profile and functionality of the substrates were confirmed by water contact angle and XPS measurements.

After 24 hours of culture, chondrocytes experienced high adhesion in amine functionalized substrates compared to hydroxyl substrates. After 7 days, a more remarkable influence of the different concentrations on cell proliferation and a higher cell number was observed in higher concentration of hydroxyl (position 2.25 mm), compared with lower concentration of amine (position 0.25). After 14 days of culture, both amine and hydroxyl functionalized surfaces induced chondrocyte phenotype maintenance, and chemical concentrations did not significantly affect this cell behavior.

Actin organization was also studied to observe cytoskeletal arrangement. Overall, chondrocytes maintained their round shape for both study groups, but in lower concentrations the actin organization was more localized towards one side of the cell, which is a similar behavior of healthy chondrocytes. In higher gradient concentrations the actin filaments looked less organized, similar to OA chondrocytes.

These results are critical in improving the expansion process of autologous harvested chondrocyte cells, as an important step on behalf of a viable tissue engineering strategy for osteoarthritis treatment.

CHAPTER VI

SUMMARY

This thesis outlines our efforts to investigate the effect of hydroxyl and amine functionalized surfaces on chondrocyte behavior aiming to optimize *in vitro* culture methods for cell expansion, facing the current challenge of cartilage tissue engineering to develop feasible large scale expansion methods. Since chondrocytes undergo the process of dedifferentiation when cultured in monolayer systems, we aimed to study conditions to increase cell number and favor phenotype maintenance. To explore the effect of the two surface chemistry concentrations, we fabricated gradient substrates by a “vacuum away” deposition method, controlled by diffusion. The samples were tested by contact angle and XPS, in order to verify the linear gradient concentration profile and the surface functionalities. The proliferative potential of the substrates was analyzed by studying human osteoarthritic chondrocyte density response as a function of the terminal group’ concentration, and phenotype maintenance was quantified by the ratio of two surface markers, namely CD14/CD90. The results show that surface chemistry has a significant impact on human chondrocyte behavior. After 7 days of culture, cell numbers were found to reach maximum density for higher concentrations of functionalized hydroxyl FCGS, while the maximum density was related to lower concentrations on amine FCGS. Both functional groups were found to promote phenotype maintenance after 14 days of culture, but chemical concentrations did not have significant impact in this assay.

REFERENCES

1. Prevalence of Doctor-Diagnosed Arthritis and Arthritis-Attributable Activity Limitation — United States, 2010–2012. Prevention, C. f. D. C. a., Ed. Morbidity and Mortality Weekly Report, 2013; Vol. 62, pp 869.
2. Chikanza, I. C.; Fernandes, L., Novel strategies for the treatment of osteoarthritis. *Expert Opinion on Investigational Drugs* **2000**, 9 (7), 1499.
3. Lorenz, H.; Richter, W., Osteoarthritis: Cellular and molecular changes in degenerating cartilage. *Progress in Histochemistry and Cytochemistry* **2006**, 40 (3), 135.
4. Quintana, J. M.; Arostegui, I.; Escobar, A.; Azkarate, J.; Goenaga, J.; Lafuente, I., PRevalence of knee and hip osteoarthritis and the appropriateness of joint replacement in an older population. *Archives of Internal Medicine* **2008**, 168 (14), 1576.
5. Osteoarthritis, Arthritis Foundation (web). (accessed March 15, 2016).
6. King, W. Treatments Options for Osteoarthritis in the Knee, Palo Alto Medical Foundation (web). (accessed October 07, 2015).
7. Centeno, C.; Pitts, J.; Al-Sayegh, H.; Freeman, M., Efficacy of Autologous Bone Marrow Concentrate for Knee Osteoarthritis with and without Adipose Graft. *BioMed Research International* **2014**, 2014.
8. Nasab, M. B.; Hassan, M. R.; Sahari, B. B., Mettalic Bimaterials of Knee and Hip - A Review. *Trends Biomater. Artif. Organs* **2010**, 24 (1), 69.
9. Zaslav, K.; Cole, B.; Brewster, R.; DeBerardino, T.; Farr, J.; Fowler, P.; Nissen, C., A Prospective Study of Autologous Chondrocyte Implantation in Patients With Failed Prior Treatment for Articular Cartilage Defect of the Knee: Results of the Study of the Treatment of Articular Repair (STAR) Clinical Trial. *The American Journal of Sports Medicine* **2009**, 37 (1), 42.
10. Parmar, P. A.; Chow, L. W.; St-Pierre, J.-P.; Horejs, C.-M.; Peng, Y. Y.; Werkmeister, J. A.; Ramshaw, J. A. M.; Stevens, M. M., Collagen-mimetic peptide-modifiable hydrogels for articular cartilage regeneration. *Biomaterials* **2015**, 54, 213.
11. Ma, Y.; Zheng, J.; Amond, E. F.; Stafford, C. M.; Becker, M. L., Facile Fabrication of “Dual Click” One- and Two-Dimensional Orthogonal Peptide Concentration Gradients. *Biomacromolecules* **2013**, 14 (3), 665.

12. Johnsen, M. B.; Hellevik, A. I.; Baste, V.; Furnes, O.; Langhammer, A.; Flugsrud, G.; Nordsletten, L.; Zwart, J. A.; Storheim, K., Leisure time physical activity and the risk of hip or knee replacement due to primary osteoarthritis: a population based cohort study (The HUNT Study). *BMC Musculoskeletal Disorders* **2016**, *17* (1), 1.
13. Pereira, D.; Peleteiro, B.; Araújo, J.; Branco, J.; Santos, R. A.; Ramos, E., The effect of osteoarthritis definition on prevalence and incidence estimates: a systematic review. *Osteoarthritis and Cartilage* **2011**, *19* (11), 1270.
14. Heidari, B., Knee osteoarthritis prevalence, risk factors, pathogenesis and features: Part I. *Caspian Journal of Internal Medicine* **2011**, *2* (2), 205.
15. Kotlarz, H.; Gunnarsson, C. L.; Fang, H.; Rizzo, J. A., Insurer and out-of-pocket costs of osteoarthritis in the US: Evidence from national survey data. *Arthritis & Rheumatism* **2009**, *60* (12), 3546.
16. Losina, E.; Paltiel, A. D.; Weinstein, A. M.; Yelin, E.; Hunter, D. J.; Chen, S. P.; Klara, K.; Suter, L. G.; Solomon, D. H.; Burbine, S. A.; Walensky, R. P.; Katz, J. N., Lifetime Medical Costs of Knee Osteoarthritis Management in the United States: Impact of Extending Indications for Total Knee Arthroplasty. *Arthritis Care & Research* **2015**, *67* (2), 203.
17. Weiss, E.; Jurmain, R., Osteoarthritis revisited: a contemporary review of aetiology. *International Journal of Osteoarchaeology* **2007**, *17* (5), 437.
18. López-Cortés, R.; Formigo, J.; Reboiro-Jato, M.; Fdez-Riverola, F.; Blanco, F. J.; Lodeiro, C.; Oliveira, E.; Capelo, J. L.; Santos, H. M., A methodological approach based on gold-nanoparticles followed by matrix assisted laser desorption ionization time of flight mass spectrometry for the analysis of urine profiling of knee osteoarthritis. *Talanta* **2016**, *150*, 638.
19. Hollander, A. P.; Dickinson, S. C.; Kafienah, W., Stem Cells and Cartilage Development: Complexities of a Simple Tissue. *Stem Cells (Dayton, Ohio)* **2010**, *28* (11), 1992.
20. Martel-Pelletier, J.; Wildi, L. M.; Pelletier, J.-P., Future therapeutics for osteoarthritis. *Bone* **2012**, *51* (2), 297.
21. Rieppo, J.; Töyräs, J.; Nieminen, M. T.; Kovanen, V.; Hyttinen, M. M.; Korhonen, R. K.; Jurvelin, J. S.; Helminen, H. J., Structure-Function Relationships in Enzymatically Modified Articular Cartilage. *Cells Tissues Organs* **2003**, *175* (3), 121.
22. Tanaka, S.; Hamanishi, C.; Kikuchi, H.; Fukuda, K., Factors related to degradation of articular cartilage in osteoarthritis: A review. *Seminars in Arthritis and Rheumatism* **1998**, *27* (6), 392.

23. Grigoloa, B.; Lisignolia, G.; Piacentinia, A.; Fiorinia, M.; Gobbib, P.; Mazzottib, G.; Ducac, M.; Pavesioc, A.; Facchinia, A., Evidence for redifferentiation of human chondrocytes grown on a hyaluronan-based biomaterial (HYAFFs11): molecular, immunohistochemical and ultrastructural analysis. *Biomaterials* **2002**, *23* (4), 1187.
24. Huey, D. J.; Hu, J. C.; Athanasiou, K. A., Unlike Bone, Cartilage Regeneration Remains Elusive. *Science* **2012**, *338* (6109), 917.
25. Ochi, M.; Uchio, Y.; Kawasaki, K.; Wakitani, S.; Iwasa, J., Transplantation of cartilage-like tissue made by tissue engineering in the treatment of cartilage defects of the knee. *Bone & Joint Journal* **2002**, *84-B* (4), 571.
26. Ebert, J. R.; Smith, A.; Fallon, M.; Butler, R.; Nairn, R.; Breidahl, W.; Wood, D. J., Incidence, Degree, and Development of Graft Hypertrophy 24 Months After Matrix-Induced Autologous Chondrocyte Implantation: Association With Clinical Outcomes. *The American Journal of Sports Medicine* **2015**, *43* (9), 2208.
27. Niethammer, T. R.; Valentin, S.; Gülecyyüz, M. F.; Roßbach, B. P.; Ficklscherer, A.; Pietschmann, M. F.; Müller, P. E., Bone Marrow Edema in the Knee and Its Influence on Clinical Outcome After Matrix-Based Autologous Chondrocyte Implantation: Results After 3-Year Follow-up. *The American Journal of Sports Medicine* **2015**, *43* (5), 1172.
28. Yodmuang, S.; McNamara, S. L.; Nover, A. B.; Mandal, B. B.; Agarwal, M.; Kelly, T.-A. N.; Chao, P.-h. G.; Hung, C.; Kaplan, D. L.; Vunjak-Novakovic, G., Silk microfiber-reinforced silk hydrogel composites for functional cartilage tissue repair. *Acta Biomaterialia* **2015**, *11*, 27.
29. Bhattacharjee, M.; Coburn, J.; Centola, M.; Murab, S.; Barbero, A.; Kaplan, D. L.; Martin, I.; Ghosh, S., Tissue engineering strategies to study cartilage development, degeneration and regeneration. *Advanced Drug Delivery Reviews* **2015**, *84*, 107.
30. Melero-Martin, J. M.; Al-Rubeai, M., In Vitro Expansion of Chondrocytes. In *Topics in Tissue Engineering*, Ashammakhi, N.; Reis, R. L.; Chiellini, E., Eds. Ireland, 2007; Vol. 3, p Chapter 2.
31. Brodtkin, K. R.; García, A. J.; Levenston, M. E., Chondrocyte phenotypes on different extracellular matrix monolayers. *Biomaterials* **2004**, *25* (28), 5929.
32. Von Der Mark, K.; Gauss, V.; Von Der Mark, H.; Muller, P., Relationship between cell shape and type of collagen synthesised as chondrocytes lose their cartilage phenotype in culture. *Nature* **1977**, *267* (5611), 531.
33. Thirion, S.; Berenbaum, F., Culture and Phenotyping of Chondrocytes in Primary Culture. In *Methods in Molecular Medicine*, Sabatini, M.; Pastoureau, P.; Ceuninck, F. d., Eds. Humana Press Inc.: 2004; Vol. 1 - Cellular and Molecular Tools, pp 1.

34. Ma, Z.; Gao, C.; Gong, Y.; Shen, J., Chondrocyte behaviors on poly-l-lactic acid (PLLA) membranes containing hydroxyl, amide or carboxyl groups. *Biomaterials* **2003**, *24* (21), 3725.
35. Phillips, J. E.; Petrie, T. A.; Creighton, F. P.; García, A. J., Human mesenchymal stem cell differentiation on self-assembled monolayers presenting different surface chemistries. *Acta Biomaterialia* **2010**, *6* (1), 12.
36. Moore, N. M.; Lin, N. J.; Gallant, N. D.; Becker, M. L., The use of immobilized osteogenic growth peptide on gradient substrates synthesized via click chemistry to enhance MC3T3-E1 osteoblast proliferation. *Biomaterials* **2010**, *31* (7), 1604.
37. Curran, J. M.; Chen, R.; Hunt, J. A., The guidance of human mesenchymal stem cell differentiation in vitro by controlled modifications to the cell substrate. *Biomaterials* **2006**, *27* (27), 4783.
38. Genzer, J.; Bhat, R. R., Surface-Bound Soft Matter Gradients. *Langmuir* **2008**, *24* (6), 2294.
39. Ren, Y.-J.; Zhang, H.; Huang, H.; Wang, X.-M.; Zhou, Z.-Y.; Cui, F.-Z.; An, Y.-H., In vitro behavior of neural stem cells in response to different chemical functional groups. *Biomaterials* **2009**, *30* (6), 1036.
40. Albert, J. N. L.; Baney, M. J.; Stafford, C. M.; Kelly, J. Y.; Epps, T. H., Generation of Monolayer Gradients in Surface Energy and Surface Chemistry for Block Copolymer Thin Film Studies. *ACS Nano* **2009**, *3* (12), 3977.
41. Gallant, N. D.; Lavery, K. A.; Amis, E. J.; Becker, M. L., Universal Gradient Substrates for "Click" Biofunctionalization. *Adv. Mater.* **2007**, *19*, 965.
42. Smith Callahan, L. A.; Childers, E. P.; Bernard, S. L.; Weiner, S. D.; Becker, M. L., Maximizing phenotype constraint and extracellular matrix production in primary human chondrocytes using arginine–glycine–aspartate concentration gradient hydrogels. *Acta Biomaterialia* **2013**, *9* (7), 7420.
43. Himo, F.; Lovell, T.; Hilgraf, R.; Rostovtsev, V. V.; Noodleman, L.; Sharpless, K. B.; Fokin, V. V., Copper(I)-Catalyzed Synthesis of Azoles. DFT Study Predicts Unprecedented Reactivity and Intermediates. *Journal of the American Chemical Society* **2005**, *127* (1), 210.
44. Heidari, M.; Tahmasebi, M. N.; Etemad, S.; Salehkhoulou, S.; Heidari-Vala, H.; Akhondi, M. M., In vitro Human Chondrocyte Culture; A Modified Protocol. *Middle-East Journal of Scientific Research* **2011**, *9* (1), 102.
45. Yang, J.; Alexander, M. R., Techniques for analysing biomaterial surface chemistry. In *Surface Modification of Biomaterials. Methods, analysis and applications.*, 1st ed.; Williams, R., Ed. Woodhead Publishing Limited: 2010; p 211.

46. Fadeev, A. Y.; McCarthy, T. J., Trialkylsilane Monolayers Covalently Attached to Silicon Surfaces: Wettability Studies Indicating that Molecular Topography Contributes to Contact Angle Hysteresis. *Langmuir* **1999**, *15* (11), 3759.
47. Li, J. E. J.; Kawazoe, N.; Chen, G., Gold nanoparticles with different charge and moiety induce differential cell response on mesenchymal stem cell osteogenesis. *Biomaterials* **2015**, *54*, 226.
48. Faucheux, N.; Schweiss, R.; Lützow, K.; Werner, C.; Groth, T., Self-assembled monolayers with different terminating groups as model substrates for cell adhesion studies. *Biomaterials* **2004**, *25* (14), 2721.
49. Lee, J. H.; Jung, H. W.; Kang, I.-K.; Lee, H. B., Cell behaviour on polymer surfaces with different functional groups. *Biomaterials* **1994**, *15* (9), 705.
50. Mahmood, T. A.; de Jong, R.; Riesle, J.; Langer, R.; van Blitterswijk, C. A., Adhesion-mediated signal transduction in human articular chondrocytes: the influence of biomaterial chemistry and tenascin-C. *Experimental Cell Research* **2004**, *301* (2), 179.
51. Adami, R.; Cintio, O.; Trombetta, G.; Choquet, D.; Grazi, E., On the stiffness of the natural actin filament decorated with alexa fluor tropomyosin. *Biophysical Chemistry* **2003**, *104* (2), 469.
52. Diaz-Romero, J.; Nestic, D.; Grogan, S. P.; Heini, P.; Mainil-Varlet, P., Immunophenotypic changes of human articular chondrocytes during monolayer culture reflect bona fide dedifferentiation rather than amplification of progenitor cells. *Journal of Cellular Physiology* **2008**, *214* (1), 75.
53. Giovannini, S.; Diaz-Romero, J.; Aigner, T.; Mainil-Varlet, P.; Nestic, D., Population doublings and percentage of S100-positive cells as predictors of in vitro chondrogenicity of expanded human articular chondrocytes. *Journal of Cellular Physiology* **2010**, *222* (2), 411.
54. Johnsen, M. B.; Hellevik, A. I.; Baste, V.; Furnes, O.; Langhammer, A.; Flugsrud, G.; Nordsletten, L.; Zwart, J. A.; Storheim, K., Leisure time physical activity and the risk of hip or knee replacement due to primary osteoarthritis: a population based cohort study (The HUNT Study). *BMC Musculoskeletal Disorders* **2016**, *17*, 86.
55. Woodfield, T. B. F.; Miot, S.; Martin, I.; van Blitterswijk, C. A.; Riesle, J., The regulation of expanded human nasal chondrocyte re-differentiation capacity by substrate composition and gas plasma surface modification. *Biomaterials* **2006**, *27* (7), 1043.